

# Irvsp: to obtain irreducible representations of electronic states in the VASP

Jiacheng Gao,<sup>1,2</sup> Quansheng Wu,<sup>3,4</sup> Clas Persson,<sup>5,6</sup> and Zhijun Wang<sup>1,2,\*</sup>

<sup>1</sup>*Beijing National Laboratory for Condensed Matter Physics,  
and Institute of Physics, Chinese Academy of Sciences, Beijing 100190, China*

<sup>2</sup>*University of Chinese Academy of Sciences, Beijing 100049, China*

<sup>3</sup>*Institute of Physics, École Polytechnique Fédérale de Lausanne, CH-1015 Lausanne, Switzerland*

<sup>4</sup>*National Centre for Computational Design and Discovery of Novel Materials MARVEL,  
Ecole Polytechnique Fédérale de Lausanne (EPFL), CH-1015 Lausanne, Switzerland*

<sup>5</sup>*Centre for Materials Science and Nanotechnology, Department of Physics,  
University of Oslo, P.O. Box 1048 Blindern, NO-0316 Oslo, Norway*

<sup>6</sup>*Department of Materials Science and Engineering,  
KTH Royal Institute of Technology, Stockholm, SE-100 44, Sweden*

We present an open-source program **irvsp**, to compute irreducible representations of electronic states for all 230 space groups with an interface to the Vienna *ab-initio* Simulation Package. This code is fed with plane-wave-based wavefunctions (*e.g.* WAVECAR) and space group operators (listed in OUTCAR), which are generated by the VASP package. This program computes the traces of matrix presentations and determines the corresponding irreducible representations for all energy bands and all the  $k$ -points in the three-dimensional Brillouin zone. It also works with spin-orbit coupling (SOC), *i.e.*, for double groups. It is in particular useful to analyze energy bands, their connectivities, and band topology, after the establishment of the theory of topological quantum chemistry. Accordingly, the associated library – **irrep\_bcs.a** – is developed, which can be easily linked to by other *ab-initio* packages. In addition, the program has been extended to orthogonal tight-binding (TB) Hamiltonians, *e.g.* electronic or phononic TB Hamiltonians. A sister program **ir2tb** is presented as well.

## Program summary

*Program title:* irvsp

*Program Files doi:* <https://doi.org/10.17632/y9ds5nm2f.1>

*Licensing provisions:* GNU Lesser General Public License, <https://www.gnu.org/licenses/lgpl-3.0.html>

*Distribution format:* tar.gz

*Programming language:* Fortran 90/77

*Computer:* Any architecture with a Fortran 90 compiler

*RAM:* 20 MB

*Nature of problem:* Determining irreducible representations for all energy bands and all the  $k$ -points in 230 space groups. It is in particular useful to analyze energy bands, their connectivities, and band topology.

*Solution method:* By computing the traces of matrix presentations of space group operators for the eigen-wavefunctions at a certain  $k$ -point in a given space group, one can determine irreducible representations for them.

*Running time:* It takes less than 1 minute for the calculation of Bismuth.

## Keywords

Irreducible representations; First-principles calculations; Nonsymmorphic space groups; Plane-wave basis; Tight-binding Hamiltonian; Topological materials

## I. INTRODUCTION

Topological states have been intensively studied in the past decades [1–9]. During the period, lots of materials have theoretically been proposed to be topological insulators and topological semimetals, based on calculations within the density-functional theory (DFT) [10–16]. Many of them are verified in experiments, and substantially intrigue much interest in theories and experiments, such as three-dimensional (3D) topological insulator Bi<sub>2</sub>Se<sub>3</sub> [17–19], Dirac semimetals Na<sub>3</sub>Bi [20, 21] and Cd<sub>3</sub>As<sub>2</sub> [22, 23], Weyl semimetal TaAs [24–27], topological crystalline insulator SnTe [28, 29] and hourglass material KHgSb [30, 31] *et al.* To some extent, these topological electron bands are related to a

---

\*Electronic address: [zjwang11@hotmail.com](mailto:zjwang11@hotmail.com);

The codes are available in the public repository: <https://github.com/zjwang11/irvsp/>.

band-inversion feature. Explicitly, there can be a band inversion between different irreducible representations (IRs) of the little groups at  $k$ -points in the 3D Brillouin zone (BZ) [32]. In the situation of Dirac semimetals or nodal-line semimetals, the band inversion may happen on a high-symmetry line or in a high-symmetry plane.

Very recently, new insights about band theory have been used to classify all the nontrivial electron band topologies compatible with a given crystal structure [33–36]. In particular, based on the theory of topological quantum chemistry (TQC) [36–39], the topology of a set of isolated electron bands is relied on IRs at the maximal high-symmetry  $k$ -points (HSK), as the compatibility relations are obtained in Ref. [40], and open accessible on the Bilbao Crystallographic Server (BCS) [41, 42]. The set of maximal HSK points can be found by using the BCS. The determination of the IRs of electron bands at maximal HSK points is of great interest, for which the program – `vasp2trace` – was developed [12]. However, it is not suitable for any non-maximal HSK points.

Generally speaking, in order to obtain the IRs for electron energy bands in crystals, two ingredients are necessary: a) wave-functions (WFs) at  $k$ -points and b) character tables (CRTs) for  $k$ -little groups. Different versions of the codes can be developed based on the different types of the WFs and conventions of the CRTs. The program `irrep` in the WIEN2k package [43, 44] is a precursor in determining the IRs, which is based on the plane-wave (PW) basis (the part of the WFs outside muffin-tin spheres) and the CRTs of 32 point groups (PNGs). There is an advantage of describing the IRs in terms of the more well-known PNG symmetries; however, the disadvantage is that in many cases  $k$ -points on the BZ surface cannot be classified with PNGs for nonsymmorphic crystals. In this paper, the program – `irvsp` – is developed based on the CRTs on the BCS. It originates from the WIEN2k `irrep` code [43, 44] that considers both single and double groups, analyses of time-reversal symmetry, and handles accidental degeneracies. The present code inherits those features but it has been extended to also be able to determine IRs of those special  $k$ -points for nonsymmorphic crystals. Hence, the code labels the IRs according to the convention of the BCS notation [42] for 230 space groups (SGs). In fact, it works for 1651 magnetic space groups (MSGs), once the space group number of the unitary part of MSGs is correctly given. In addition, Wannier-based tight-binding (TB) models are widely used to study the topological properties of real materials, including topological surface states and symmetry indicators. To get the band representations and check the topology of these models, a sister program – `ir2tb` – is developed to interface with orthogonal TB Hamiltonians, *e.g.* electronic or phononic TB Hamiltonians.

This paper is organized as follows. In Section II, we present some basic derivations to compute the traces of matrix presentations (MPs) in different bases. In Section III, we introduce the general process of the code. In Section IV, we introduce the capabilities of this package. In Section V, we introduce the installation and basic usages. In Section VI, we introduce some examples in order to show how to use `irvsp` to determine the IRs and further explore the topology.

## II. METHODS

Space-group operations (SGOs),  $\mathcal{O}_s = \{R_s|\mathbf{v}_s\}$ , consist of two parts: a rotation part  $R_s$  and a translation part  $\mathbf{v}_s$ . The product of two operations is defined as  $\{R_s|\mathbf{v}_s\}\{R_t|\mathbf{v}_t\} = \{R_s R_t|R_s \mathbf{v}_t + \mathbf{v}_s\}$ . An operator acting on a scalar function in real space is expressed by  $\mathcal{O}_s f(\mathbf{r}) = f(\mathcal{O}_s^{-1} \mathbf{r}) = f(R_s^{-1} \mathbf{r} - R_s^{-1} \mathbf{v}_s)$  (There is a typo in Section A of the supplementary information of Ref. [12]). The MPs,  $O_s^{mn}$ , can be computed in the basis of the Bloch wavefunctions  $|\psi_{n\mathbf{k}}\rangle$ :  $O_s^{mn} = \langle \psi_{m\mathbf{k}} | \mathcal{O}_s | \psi_{n\mathbf{k}} \rangle$ . The traces of the obtained MPs are the characters, and they are essential to determine the corresponding IRs of the little group (LG) of  $\mathbf{k}$ . The LG of  $\mathbf{k}$  [ $LG(k)$ ] is defined as a set of SGOs:

$$LG(k) : \{ \mathcal{O}_s | R_s \mathbf{k} = \mathbf{k} + \mathbf{G} \}, \text{ with } \mathbf{G} = l\mathbf{g}_1 + m\mathbf{g}_2 + n\mathbf{g}_3, \quad l, m, n \in \mathbb{N} \quad (1)$$

Here,  $\mathbf{G}$  could be any integer reciprocal lattice translation ( $\mathbf{g}_1, \mathbf{g}_2, \mathbf{g}_3$  are primitive reciprocal lattice vectors). The traces of MPs of SGOs are defined as:

$$\text{Tr}[\mathcal{O}_s] = \sum_n O_s^{nn} \text{ with } O_s^{nn} = \langle \psi_{n\mathbf{k}} | \mathcal{O}_s | \psi_{n\mathbf{k}} \rangle, \quad \mathcal{O}_s \in LG(k). \quad (2)$$

Here, the WFs have to be normalized (*i.e.*,  $\langle \psi_{n\mathbf{k}} | \psi_{n\mathbf{k}} \rangle = 1$ ).

Under different bases, the WFs can be expressed in different ways, and the derivations of Eq. (2) are different. Here, we have derived the expressions in two bases: i) PW basis and ii) TB basis. In what follows, symbols in the bold text are vectors, and common bracket notations are employed:

$$\begin{aligned} \langle \mathbf{r} | A \rangle &\equiv A(\mathbf{r}) \\ \langle A | B \rangle &\equiv \int d\mathbf{r} A^*(\mathbf{r}) B(\mathbf{r}) \\ \langle \mathbf{r} | \mathbf{k} \rangle &\equiv e^{i\mathbf{k} \cdot \mathbf{r}} \end{aligned}$$

To be convenient, we present the derivations in the cases without the spin degree of freedom. However, the derivations can be easily extended to the cases including SOC, by substituting  $R_s \otimes SU_s(2)$  for  $R_s$ , where the bases are doubled by the direct product:  $\{\text{PW/TB basis}\} \otimes \{|\uparrow\rangle, |\downarrow\rangle\}$ . In fact, the code works for both single and double groups.

### A. Plane-wave basis

In the PW basis, wavefunctions/eigenstates are expressed in the basis of plane waves:

$$\psi_{n\mathbf{k}}(\mathbf{r}) = \sum_j C_{\mathbf{k},j} e^{i(\mathbf{k}+\mathbf{G}_j)\cdot\mathbf{r}} \text{ with } \langle \mathbf{k} + \mathbf{G}_i | \mathbf{k} + \mathbf{G}_j \rangle = \delta_{ij} \quad (3)$$

The coefficients ( $C_{\mathbf{k},j}$ ) are usually computed in the *ab-initio* calculations and output by the DFT package (*e.g.* VASP, PWscf, *etc.*). The SGOs acting on WFs are derived as:

$$\begin{aligned} \mathcal{O}_s \psi_{n\mathbf{k}}(\mathbf{r}) &= \sum_j C_{\mathbf{k},j} e^{i(\mathbf{k}+\mathbf{G}_j)\cdot(R_s^{-1}\mathbf{r}-R_s^{-1}\mathbf{v}_s)} \\ &= \sum_j C_{\mathbf{k},j} e^{iR_s(\mathbf{k}+\mathbf{G}_j)\cdot(\mathbf{r}-\mathbf{v}_s)} \\ &= \sum_j C_{\mathbf{k},j} e^{i(\mathbf{k}+\mathbf{G}_{j'})\cdot(\mathbf{r}-\mathbf{v}_s)} \text{ with } \mathbf{k} + \mathbf{G}_{j'} \equiv R_s(\mathbf{k} + \mathbf{G}_j) \\ &= e^{-i\mathbf{k}\cdot\mathbf{v}_s} \sum_j C_{\mathbf{k},j} e^{-i\mathbf{G}_{j'}\cdot\mathbf{v}_s} e^{i(\mathbf{k}+\mathbf{G}_{j'})\cdot\mathbf{r}} \text{ with } \mathbf{G}_{j'} \equiv R_s(\mathbf{k} + \mathbf{G}_j) - \mathbf{k} \end{aligned}$$

Then, Eq. (2) can be written as:

$$\langle \psi_{n\mathbf{k}} | \mathcal{O}_s | \psi_{n\mathbf{k}} \rangle = e^{-i\mathbf{k}\cdot\mathbf{v}_s} \sum_j C_{\mathbf{k},j}^* C_{\mathbf{k},j} e^{-i\mathbf{G}_{j'}\cdot\mathbf{v}_s} \text{ with } \mathbf{G}_{j'} \equiv R_s(\mathbf{k} + \mathbf{G}_j) - \mathbf{k} \quad (4)$$

The program `irvsp` is developed based on the above derivations with the interface to VASP [45]. In addition, the library of the code is developed (see details in Appendix 6), which can be downloaded from the public code archive: [https://github.com/zjwang11/irvsp/blob/master/lib\\_irrep\\_bcs.tar.gz](https://github.com/zjwang11/irvsp/blob/master/lib_irrep_bcs.tar.gz). The library – `irrep_bcs.a` – can be easily linked to by other *ab-initio* packages, once a proper interface is made.

### B. Orthogonal tight-binding basis

In a TB Hamiltonian, WFs are expressed in the basis of exponentially localized orthogonal orbitals:  $|\mathbf{0}, \mu\alpha\rangle \equiv \phi_\alpha^\mu(\mathbf{r}) \equiv \phi_\alpha(\mathbf{r} - \tau_\mu)$  and  $|\mathbf{L}_j, \mu\alpha\rangle \equiv \phi_\alpha(\mathbf{r} - \mathbf{L}_j - \tau_\mu)$ , where  $\mu$  label the atoms,  $\alpha$  label the orbitals,  $\mathbf{L}_j$  label the lattice vectors in 3D crystals, and  $\tau_\mu$  label the positions of atoms in the home unit cell. At a given  $k$ -point, WFs are given as:

$$\psi_{n\mathbf{k}}(\mathbf{r}) = \sum_{\mu\alpha} C_{\mu\alpha,\mathbf{k}}^n \phi_{\alpha\mathbf{k}}^\mu(\mathbf{r}) \text{ where } n \text{ is a band index,} \quad (5)$$

$$\phi_{\alpha\mathbf{k}}^\mu(\mathbf{r}) = \sum_j \phi_\alpha(\mathbf{r} - \tau_\mu - \mathbf{L}_j) e^{i\mathbf{k}\cdot(\mathbf{L}_j + \tau_\mu)}, \left\langle \phi_{\beta\mathbf{k}}^{\mu'} | \phi_{\alpha\mathbf{k}}^\mu \right\rangle = \delta_{\mu\mu'} \delta_{\alpha\beta} \quad (6)$$

The states  $\phi_{\alpha\mathbf{k}}^\mu(\mathbf{r})$  are the Fourier transformations of the local orbitals  $\phi_\alpha^\mu(\mathbf{r})$ , as shown in Eq. (6). The coefficients are obtained as the eigenvectors of the TB Hamiltonian:  $H_{\mu'\beta,\mu\alpha}(\mathbf{k}) = \sum_j e^{i\mathbf{k}\cdot(\mathbf{L}_j + \tau_\mu - \tau_{\mu'})} \left\langle \mathbf{0}, \mu'\beta | \hat{H} | \mathbf{L}_j, \mu\alpha \right\rangle$ . The rotational symmetries  $R_s$  acting on the local orbitals  $[\phi_\alpha(\mathbf{r})]$  at the  $\mu$  site are given as:

$$\widehat{R_s} \phi_\alpha(\mathbf{r}) \equiv R_s \phi_\alpha(\mathbf{r}) = \sum_\beta \phi_\beta(\mathbf{r}) D_{\beta\alpha}^{s,\mu} \quad (7)$$

These  $D$ -matrices are explicitly given in Table S3 in Appendix 2. Under the basis of real spherical harmonic functions with different total angular momenta (integer  $l$ ), these  $D$ -matrices are real.

The SGOs acting on the states  $\phi_{\alpha\mathbf{k}}^\mu(\mathbf{r})$  are given below:

$$\begin{aligned}
\mathcal{O}_s \phi_{\alpha\mathbf{k}}^\mu(\mathbf{r}) &= \phi_{\alpha\mathbf{k}}^\mu(R_s^{-1}\mathbf{r} - R_s^{-1}\mathbf{v}_s) \\
&= \sum_j \phi_\alpha(R_s^{-1}\mathbf{r} - R_s^{-1}\mathbf{v}_s - \tau_\mu - \mathbf{L}_j) e^{i\mathbf{k}\cdot(\mathbf{L}_j + \tau_\mu)} \\
&= \sum_j \phi_\alpha(R_s^{-1}[\mathbf{r} - \mathbf{v}_s - R_s\tau_\mu - R_s\mathbf{L}_j]) e^{i\mathbf{k}\cdot(\mathbf{L}_j + \tau_\mu)} \\
&= \sum_j \widehat{R_s\phi}_\alpha[\mathbf{r} - \mathbf{v}_s - R_s\tau_\mu - R_s\mathbf{L}_j] e^{i(R_s\mathbf{k})\cdot R_s(\mathbf{L}_j + \tau_\mu)} \text{ with } \widehat{R_s\phi}_\alpha(\mathbf{r}) \equiv \sum_\beta \phi_\beta(\mathbf{r}) D_{\beta\alpha}^{s,\mu} \\
&= e^{-i(R_s\mathbf{k}\cdot\mathbf{v}_s)} \sum_j \widehat{R_s\phi}_\alpha[\mathbf{r} - (\mathbf{v}_s + R_s\tau_\mu) - R_s\mathbf{L}_j] e^{i(R_s\mathbf{k})\cdot[R_s\mathbf{L}_j + (R_s\tau_\mu + \mathbf{v}_s)]} \\
&= e^{-i(R_s\mathbf{k}\cdot\mathbf{v}_s)} \sum_j \widehat{R_s\phi}_\alpha[\mathbf{r} - (\tau_{\mu'} + \mathbf{L}_0^i) - R_s\mathbf{L}_j] e^{i(R_s\mathbf{k})\cdot[R_s\mathbf{L}_j + (\tau_{\mu'} + \mathbf{L}_0^i)]} \text{ using } \mathbf{v}_s + R_s\tau_\mu = \mathbf{L}_0^i + \tau_{\mu'} \\
&= e^{-i(R_s\mathbf{k}\cdot\mathbf{v}_s)} \sum_{j'} \widehat{R_s\phi}_\alpha[\mathbf{r} - \tau_{\mu'} - \mathbf{L}_{j'}] e^{i(R_s\mathbf{k})\cdot[\mathbf{L}_{j'} + \tau_{\mu'}]} \text{ with } \mathbf{L}_{j'} = \mathbf{L}_0^i + R_s\mathbf{L}_j \\
&= e^{-i(R_s\mathbf{k}\cdot\mathbf{v}_s)} \sum_\beta \phi_{\beta,R_s\mathbf{k}}^{\mu'}(r) D_{\beta\alpha}^{s,\mu}
\end{aligned}$$

Thus, Eq. (2) is written as:

$$\langle \psi_{n\mathbf{k}} | \mathcal{O}_s | \psi_{n\mathbf{k}} \rangle = e^{-i(R_s\mathbf{k}\cdot\mathbf{v}_s)} \sum_{\alpha\mu,\beta} (C_{\mu'\beta}^n)^* e^{i(R_s\mathbf{k}-\mathbf{k})\cdot\tau_{\mu'}} D_{\beta\alpha}^{s,\mu} C_{\mu\alpha}^n \text{ with } \mathbf{v}_s + R_s\tau_\mu = \mathbf{L}_0^i + \tau_{\mu'} \quad (8)$$

In a matrix format,

$$\langle \psi_{n\mathbf{k}} | \mathcal{O}_s | \psi_{n\mathbf{k}} \rangle = e^{-i(R_s\mathbf{k}\cdot\mathbf{v}_s)} \left[ \overline{C^\dagger V(R_s\mathbf{k} - \mathbf{k}) DC} \right]_{nn} \quad (9)$$

$$\text{with } \overline{V}(\mathbf{k})_{\mu'\beta,\mu\alpha} = e^{i\mathbf{k}\cdot\tau_\mu} \delta_{\mu\mu'} \delta_{\alpha\beta}, \quad \overline{C}_{\mu\alpha,n} = C_{\mu\alpha}^n, \quad \overline{D}_{\mu'\beta,\mu\alpha} = \begin{cases} D_{\beta\alpha}^{s,\mu} & \text{when } \mathbf{v}_s + R_s\tau_\mu = \mathbf{L}_0^i + \tau_{\mu'}; \\ 0 & \text{otherwise.} \end{cases} \quad (10)$$

Based on the above derivations, the code has been extended to the TB basis. The sister program is called **ir2tb**. To run **ir2tb**, users must provide two files: **case\_hr.dat** and **tbbox.in**. The file called **case\_hr.dat**, containing the TB parameters, may be generated by the software Wannier90 [46, 47] with symmetrization [48–50], or generated by users with a toy TB model, or generated from Slater-Koster method [51] or discretization of  $k \cdot p$  model onto a lattice [52]. The other file **tbbox.in** is the master input file for **ir2tb**. It should be given consistently with the TB parameters in **case\_hr.dat**. The **tbbox.in** for  $\text{Bi}_2\text{Se}_3$  is given in Appendix 1. In addition, the example of electronic TB Hamiltonian for  $\text{Bi}_2\text{Se}_3$  and the example of phononic TB Hamiltonian for  $\text{CoSi}$  are included in the archive **src\_ir2tb\_v2.tar.gz**.

TABLE I: A brief summary of key subroutines

File	Description	Input
<b>wave_data.f90</b>	reading the coefficients $C_{\mathbf{k},j}$ .	WAVECAR
<b>init.f90</b>	reading lattice vectors and space group operators, and setting up the $Z$ and $Z^{-1}$ matrices.	OUTCAR
<b>kgroup.f90</b>	determining the $\mathbf{k}$ -little groups.	
<b>nonsymm.f90</b>	retrieving the character tables from the BCS	
<b>chrct.f90</b>	computing the traces through Eq. (4), and determining the IRs	

### III. GENERAL PROCESS OF THE CODE

In the main text, we are mainly focused on **irvsp**, which is based on the PW basis with an interface to the VASP package [45]. The key subroutines are summarized in Table I. One can check more details for **ir2tb** and **irrep\_bcs.a**

in the Appendix. The program `ir2tb` works for orthogonal TB Hamiltonians, *e.g.* the electronic or phononic TB Hamiltonians. The library `irrep.bcs.a` can be linked to by other DFT packages.

### A. Wavefunctions at $k$ -points

In the VASP package, the all-electron wave-function is obtained by acting a linear operator  $\mathcal{T}$  on the pseudo-wavefunction:  $|\psi_{n\mathbf{k}}\rangle = \mathcal{T}|\tilde{\psi}_{n\mathbf{k}}\rangle$ . The linear operator can be written explicitly as:  $\mathcal{T} = \mathbf{1} + \sum_i (|\phi_i\rangle - |\tilde{\phi}_i\rangle)\langle p_i|$ , where  $|\phi_i\rangle$  ( $|\tilde{\phi}_i\rangle$ ) is a set of all-electron (pseudo) partial waves around each atom and  $|p_i\rangle$  is a set of corresponding projector functions on each atom within an augmentation region ( $r < R_0$ ), where  $R_0$  is the core part for each atom. The pseudo-wavefunction is expanded in the plane waves:

$$\tilde{\psi}_{n\mathbf{k}}(\vec{r}) \equiv \langle \vec{r} | \tilde{\psi}_{n\mathbf{k}} \rangle = \sum_{\mathbf{G}_j} C_{n,\mathbf{k}+\mathbf{G}_j} e^{i(\mathbf{k}+\mathbf{G}_j)\cdot\vec{r}} \quad (11)$$

where  $\mathbf{G}_j$  vectors are determined by the condition  $\frac{\hbar^2}{2m_e}(\mathbf{k} + \mathbf{G}_j)^2 < E_{cutoff}$  with a cutoff  $E_{cutoff}$ . It is worthy noting that  $|\tilde{\psi}_{n\mathbf{k}}\rangle$  are sufficient for the calculations of the traces of MPs of SGOs.

Since the pseudo-wavefunctions  $|\tilde{\psi}_{n\mathbf{k}}\rangle$  are usually not normalized, they have to be renormalized before their traces can be computed via Eq. (2). The coefficients ( $C_{\mathbf{k}+\mathbf{G}_j}$ ) are output in WAVECAR by VASP. In the program, they are read by the subroutine: `wave_data.f90`. In the SOC case, the  $C_{\mathbf{k}+\mathbf{G}_j,\uparrow}$  and  $C_{\mathbf{k}+\mathbf{G}_j,\downarrow}$  are stored in the complex variables `coeffa(:)` and `coeffb(:)`. In the case without SOC, the  $C_{\mathbf{k}+\mathbf{G}_j}$  are stored in `coeffa(:)`, while `coeffb(:)` are invalid (set to be zero).

### B. Space group operators of a 3D crystal

Instead of generating space group operators from a 3D crystal structure (*i.e.*, POSCAR), the program reads the SGOs directly from the standard output of VASP (*i.e.*, OUTCAR), which is done by the subroutine: `init.f90`. In other words, the SGOs are generated by the VASP package (*e.g.* with `ISYM = 1` or `2` in INCAR for vasp.5.3.3), which are listed below the line of ‘Space group operators:’ in OUTCAR. Fig. 1 shows an example of  $\text{Bi}_2\text{Se}_3$  for the SGOs of space group (SG) 166. They are given by  $Det (\pm 1)$ ,  $\omega$ , and  $\vec{n} (n_x, n_y, n_z)$  and  $\mathbf{v} (v_1\mathbf{t}_1, v_2\mathbf{t}_2, v_3\mathbf{t}_3)$  with  $\mathbf{t}_1, \mathbf{t}_2, \mathbf{t}_3$  primitive lattice vectors. The  $-1$  value of  $Det$  indicates that the operator is a roto-inversion. Actually, the listed SGOs depend on the lattice vectors. Primitive lattice vectors ( $\mathbf{t}_1, \mathbf{t}_2, \mathbf{t}_3$ ) and primitive reciprocal lattice vectors ( $\mathbf{g}_1, \mathbf{g}_2, \mathbf{g}_3$ ) are read from OUTCAR, also shown in Fig. 2 for  $\text{Bi}_2\text{Se}_3$ . It’s worth noting that to be compatible with the CRTs in the BCS, the POSCAR should be given in a standard way (see more details in Appendix 3). The  $O(3)$  and  $SU(2)$  MPs are generated in the spin-1 (under the basis of  $\{\mathbf{x}, \mathbf{y}, \mathbf{z}\}$ ) and spin-1/2 (under the basis of  $\{\uparrow, \downarrow\}$ ) spaces, respectively:

$$R(\omega, \vec{n}) = Det \cdot e^{-i\omega(\vec{n}\cdot\vec{L})}, L_x = \begin{pmatrix} 0 & 0 & 0 \\ 0 & 0 & -i \\ 0 & i & 0 \end{pmatrix}, L_y = \begin{pmatrix} 0 & 0 & i \\ 0 & 0 & 0 \\ -i & 0 & 0 \end{pmatrix}, L_z = \begin{pmatrix} 0 & -i & 0 \\ i & 0 & 0 \\ 0 & 0 & 0 \end{pmatrix}; \quad (12)$$

$$S(\omega, \vec{n}) = e^{-i\omega(\vec{n}\cdot\vec{S})}, S_x = \frac{\sigma_x}{2} = \frac{1}{2} \begin{pmatrix} 0 & 1 \\ 1 & 0 \end{pmatrix}, S_y = \frac{\sigma_y}{2} = \frac{1}{2} \begin{pmatrix} 0 & -i \\ i & 0 \end{pmatrix}, S_z = \frac{\sigma_z}{2} = \frac{1}{2} \begin{pmatrix} 1 & 0 \\ 0 & -1 \end{pmatrix}. \quad (13)$$

In 3D crystals, it is more convenient to use MPs in the lattices of  $(\mathbf{t}_1, \mathbf{t}_2, \mathbf{t}_3)$  in real space and in reciprocal lattices of  $(\mathbf{g}_1, \mathbf{g}_2, \mathbf{g}_3)$  in momentum space. They are given in the following convention:

$$\vec{v} = \mathbf{t}_1 v_1 + \mathbf{t}_2 v_2 + \mathbf{t}_3 v_3 = (\mathbf{t}_1, \mathbf{t}_2, \mathbf{t}_3) \begin{pmatrix} v_1 \\ v_2 \\ v_3 \end{pmatrix}, (\mathbf{t}_1, \mathbf{t}_2, \mathbf{t}_3) \equiv \begin{pmatrix} t_{1x} & t_{1y} & t_{1z} \\ t_{2x} & t_{2y} & t_{2z} \\ t_{3x} & t_{3y} & t_{3z} \end{pmatrix}; \quad (14)$$

$$\vec{k} = k_1 \mathbf{g}_1 + k_2 \mathbf{g}_2 + k_3 \mathbf{g}_3 = (k_1, k_2, k_3) \begin{pmatrix} \mathbf{g}_1 \\ \mathbf{g}_2 \\ \mathbf{g}_3 \end{pmatrix}, \begin{pmatrix} \mathbf{g}_1 \\ \mathbf{g}_2 \\ \mathbf{g}_3 \end{pmatrix} \equiv \begin{pmatrix} g_{1x} & g_{1y} & g_{1z} \\ g_{2x} & g_{2y} & g_{2z} \\ g_{3x} & g_{3y} & g_{3z} \end{pmatrix}. \quad (15)$$

$$\text{with } \begin{pmatrix} \mathbf{g}_1 \\ \mathbf{g}_2 \\ \mathbf{g}_3 \end{pmatrix} (\mathbf{t}_1, \mathbf{t}_2, \mathbf{t}_3) = 2\pi \mathbb{I}_{3 \times 3}$$

Space group operators:

iropt	det(A)	alpha	n_x	n_y	n_z	tau_x	tau_y	tau_z
1	1.000000	0.000000	1.000000	0.000000	0.000000	0.000000	0.000000	0.000000
2	-1.000000	0.000000	1.000000	0.000000	0.000000	0.000000	0.000000	0.000000
3	1.000000	180.000000	0.866025	0.500000	0.000000	0.000000	0.000000	0.000000
4	-1.000000	180.000000	0.866025	0.500000	0.000000	0.000000	0.000000	0.000000
5	1.000000	120.000000	0.000000	0.000000	-1.000000	0.000000	0.000000	0.000000
6	-1.000000	120.000000	0.000000	0.000000	-1.000000	0.000000	0.000000	0.000000
7	1.000000	179.999999	0.000000	1.000000	0.000000	0.000000	0.000000	0.000000
8	-1.000000	179.999999	0.000000	1.000000	0.000000	0.000000	0.000000	0.000000
9	1.000000	120.000000	0.000000	0.000000	1.000000	0.000000	0.000000	0.000000
10	-1.000000	120.000000	0.000000	0.000000	1.000000	0.000000	0.000000	0.000000
11	1.000000	180.000000	0.866025	-0.500000	0.000000	0.000000	0.000000	0.000000
12	-1.000000	180.000000	0.866025	-0.500000	0.000000	0.000000	0.000000	0.000000

FIG. 1: Screenshot of OUTCAR, showing the space group operators of  $\text{Bi}_2\text{Se}_3$  generated by VASP.

direct lattice vectors			reciprocal lattice vectors		
1.194537707	-2.069000000	9.546666657	0.139523990	-0.241662639	0.034916201
1.194537707	2.069000000	9.546666657	0.139523990	0.241662639	0.034916201
-2.389075414	0.000000000	9.546666657	-0.279047979	0.000000000	0.034916201

FIG. 2: Screenshot of OUTCAR, showing the lattice vectors and reciprocal lattice vectors of  $\text{Bi}_2\text{Se}_3$  which are used in VASP.

The rotational symmetry operators acting on the vectors are transformed as:

$$R\vec{v} = (\mathbf{t}_1, \mathbf{t}_2, \mathbf{t}_3)Z \begin{pmatrix} v_1 \\ v_2 \\ v_3 \end{pmatrix}, \quad R\vec{k} = (k_1, k_2, k_3)Z^{-1} \begin{pmatrix} \mathbf{g}_1 \\ \mathbf{g}_2 \\ \mathbf{g}_3 \end{pmatrix}; \quad (16)$$

$$R(\mathbf{t}_1, \mathbf{t}_2, \mathbf{t}_3) = (\mathbf{t}_1, \mathbf{t}_2, \mathbf{t}_3)Z \Rightarrow Z \equiv (\mathbf{t}_1, \mathbf{t}_2, \mathbf{t}_3)^{-1}R(\mathbf{t}_1, \mathbf{t}_2, \mathbf{t}_3) \quad (17)$$

Thus, rotational MPs in the lattice vectors are  $3 \times 3$  integer matrices ( $Z$ ), which are defined in Eq. (17). Instead of the real  $R$ -matrices in Cartesian coordinates in Eq. (12), the integer matrices,  $Z$  and  $Z^{-1}$ , are actually stored and used throughout the code, which are all set in the subroutine: `init.f90`.

If one wants to do some sub-space-group symmetry calculations, one can modify the SGOs in OUTCAR and give the correct space group number accordingly. For example, if one only wants to know parity eigenvalues of the energy bands, one can change the list of SGOs with only two lines (*i.e.*, identity and inversion symmetry) and give space group #2 to run `irvsp`.

### C. Little group of a certain $k$ -point

The eigen-wavefunctions at a certain  $k$ -point only support the IRs of the little group of  $\mathbf{k}$ ,  $LG(k)$ . Therefore, for any given  $k$ -point, the program has to determine the  $\mathbf{k}$ -little group  $LG(k)$  first. This is done in the subroutine: `kgroup.f90`. The  $LG(k)$  are defined by Eq. (1). In the program, the integer matrices  $Z^{-1}$  and Eq. (16) in momentum space are used.

### D. Character tables for $\mathbf{k}$ -little groups

Currently, there are two conventions of CRTs for  $k$ -little groups. In the first convention, the  $k$  points are labeled by the IRs of the PNGs, since IRs of the space group can be expressed as IRs of the corresponding point group multiplied by a phase factor. They are suitable either for symmorphic SGs, or the inner  $k$ -points (not on the BZ boundary/surface) for the non-symmorphic SGs. The CRTs of PNGs are given in the Ref. [53, 54], which have been implemented in the program `irrep` of the WIEN2k package [43, 44]. In the second convention, all the CRTs for  $k$ -points of all 230 SGs are listed on the BCS [42]. Therefore, the program `irvsp` works for all  $k$ -points in 230 SGs. The CRTs are retrieved from the inputs of the BCS, which is done by the subroutine: `nonsymm.f90`.

As an example, consider the  $\Gamma$  point of  $\text{Bi}_2\text{Se}_3$ . Fig. 3 shows the CRT of the point group  $D_{3d}$  in the PNG convention. Fig. 4 shows the CRT in the BCS convention. Both tables can be used to determine the IRs at  $\Gamma$  in SG 166. In the table of Fig. 4, the first and two columns show the reality and the BCS labels of IRs, respectively. The following



columns indicate the characters of different SGOs. The reality of an IR is given by the definition [53, 54]:

$$\frac{1}{|G|} \sum_{j=1}^{|G|} \chi(G_j^2) = \begin{cases} 1 & \text{potentially real, case (a)} \\ 0 & \text{essentially complex, case (b)} \\ -1 & \text{pseudo-real, case (c)} \end{cases} \quad (18)$$

where  $G_j$  is an element of the group  $G$ , and  $|G|$  is the rank of the group  $G$ . In a MSG, the group  $G$  is defined as the unitary part of the MSG. In case (a), the IR is equivalent to its complex representation, and also equivalent to a real representation. In case (b), the IR is not equivalent to its complex representation. In case (c), the IR is equivalent to its complex representation, but not to a real representation.

In the type-II MSGs, including pure time-reversal symmetry (TRS), the existence of anti-unitary SGOs in the  $k$ -little group is indicated at the beginning of the character table (Fig. 4). In the absence of SOC (integer spin), TRS doubles the degeneracy of IRs in cases (b) and (c); while in the presence of SOC (half-integer spin), it doubles the degeneracy of the IRs in cases (a) and (b).

The point group is D3d  
12 symmetry operations in 6 classes  
Table 55 on page 58 in Koster et al [7]  
Table 42.4 on page 371 in Altmann et al [8]

		E	2C3	3C2	I	2IC3	3IC2
G1+	A1g	1	1	1	1	1	1
G2+	A2g	1	1	-1	1	1	-1
G3+	Eg	2	-1	0	2	-1	0
G1-	A1u	1	1	1	-1	-1	-1
G2-	A2u	1	1	-1	-1	-1	1
G3-	Eu	2	-1	0	-2	1	0

---

G4+	E1/2g	2	1	0	2	1	0
G5+	1E3/2g	1	-1	i	1	-1	i
G6+	2E3/2g	1	-1	-i	1	-1	-i
G4-	E1/2u	2	1	0	-2	-1	0
G5-	1E3/2u	1	-1	i	-1	1	-i
G6-	2E3/2u	1	-1	-i	-1	1	i

FIG. 3: The character table of point group  $D_{3d}$ , which is used to determine the IRs (*i.e.*, PNG convention) for the energy bands at  $\Gamma$  of  $\text{Bi}_2\text{Se}_3$  in **irrep** of the WIEN2k package.

The k-point name is GM  
12 symmetry operations (module lattice translations) in the GM-little group of space group 166  
We do NOT classify the elements into classes.  
Tables can be found on website: <http://www.cryst.ehu.es/>.

1	GM : kname	0.00 0.00 0.00	0.00 0.00 0.00	0.00 0.00 0.00	0.00 0.00 0.00	0.00 0.00 0.00	0.00 0.00 0.00	0.00 0.00 0.00	0.00 0.00 0.00	0.00 0.00 0.00	0.00 0.00 0.00	0.00 0.00 0.00	0.00 0.00 0.00
1	GM1+	1.00+0.00i	1.00+0.00i	1.00+0.00i	1.00+0.00i	1.00+0.00i	1.00+0.00i	1.00+0.00i	1.00+0.00i	1.00+0.00i	1.00+0.00i	1.00+0.00i	1.00+0.00i
1	GM1-	1.00+0.00i	1.00+0.00i	1.00+0.00i	1.00+0.00i	1.00+0.00i	1.00+0.00i	1.00+0.00i	1.00+0.00i	1.00+0.00i	1.00+0.00i	1.00+0.00i	1.00+0.00i
1	GM2+	1.00+0.00i	1.00+0.00i	1.00+0.00i	-1.00+0.00i	-1.00+0.00i	-1.00+0.00i	1.00+0.00i	1.00+0.00i	1.00+0.00i	1.00+0.00i	-1.00+0.00i	-1.00+0.00i
1	GM2-	1.00+0.00i	1.00+0.00i	1.00+0.00i	-1.00+0.00i	-1.00+0.00i	-1.00+0.00i	1.00+0.00i	1.00+0.00i	1.00+0.00i	1.00+0.00i	-1.00+0.00i	-1.00+0.00i
1	GM3+	2.00+0.00i	-1.00+0.00i	-1.00+0.00i	0.00+0.00i	0.00+0.00i	0.00+0.00i	2.00+0.00i	-1.00+0.00i	-1.00+0.00i	0.00+0.00i	0.00+0.00i	0.00+0.00i
1	GM3-	2.00+0.00i	-1.00+0.00i	-1.00+0.00i	0.00+0.00i	0.00+0.00i	0.00+0.00i	-2.00+0.00i	1.00+0.00i	1.00+0.00i	0.00+0.00i	0.00+0.00i	0.00+0.00i

---

0	GM4	1.00+0.00i	-1.00+0.00i	-1.00+0.00i	0.00-1.00i	0.00+1.00i	0.00-1.00i	1.00+0.00i	-1.00+0.00i	-1.00+0.00i	0.00-1.00i	0.00+1.00i	0.00-1.00i
0	GM5	1.00+0.00i	-1.00+0.00i	-1.00+0.00i	0.00+1.00i	0.00-1.00i	0.00+1.00i	1.00+0.00i	-1.00+0.00i	-1.00+0.00i	0.00+1.00i	0.00-1.00i	0.00+1.00i
0	GM6	1.00+0.00i	-1.00+0.00i	-1.00+0.00i	0.00-1.00i	0.00+1.00i	0.00-1.00i	-1.00+0.00i	1.00+0.00i	1.00+0.00i	0.00-1.00i	0.00+1.00i	0.00+1.00i
0	GM7	1.00+0.00i	-1.00+0.00i	-1.00+0.00i	0.00+1.00i	0.00-1.00i	0.00+1.00i	-1.00+0.00i	1.00+0.00i	1.00+0.00i	0.00-1.00i	0.00+1.00i	0.00-1.00i
-1	GM8	2.00+0.00i	1.00+0.00i	1.00+0.00i	0.00+0.00i	0.00+0.00i	0.00+0.00i	2.00+0.00i	1.00+0.00i	1.00+0.00i	0.00+0.00i	0.00+0.00i	0.00+0.00i
-1	GM9	2.00+0.00i	1.00+0.00i	1.00+0.00i	0.00+0.00i	0.00+0.00i	0.00+0.00i	-2.00+0.00i	-1.00+0.00i	-1.00+0.00i	0.00+0.00i	0.00+0.00i	0.00+0.00i

FIG. 4: The character table of  $\Gamma$ -little group in SG 166 on the BCS, which is used to determine the IRs (*i.e.*, BCS convention) for the energy bands at  $\Gamma$  of  $\text{Bi}_2\text{Se}_3$  in the program **irvsp**.

### E. Determination of irreducible representations

After the normalization of the PW-based pseudo-wavefunctions in VASP, the traces of MPs of SGOs can be computed via Eq. (4), which are done in the subroutine **chrct.f90**. By comparing the obtained traces and the characters of the CRTs, the IRs can be determined (see different versions in Appendix 5).

## IV. CAPABILITIES OF IRVSP

In the study of the properties of a material, the determination of IRs of computed electron bands is of great interest to diagnose the band crossing/anti-crossing, degeneracy and band topology. In the WIEN2k package, the program

**irrep** classifies the IRs in PNG symmetries, which then excludes the possibility to describe certain BZ surface  $k$ -points for nonsymmorphic crystals. Therefore, the demand to determine the IRs for all the  $k$ -point in all 230 SGs is still unsatisfied. With the CRTs from the BCS, the program – **irvsp** – is developed to meet this demand with the interface to the VASP package. The associated library – **irrep\_bcs.a** – can be easily linked to by other *ab-initio* packages. The obtained IRs are labeled in the convention of the BCS notation, which can be directly compared with the elementary band representations (EBRs) of the TQC theory, to further check the topology of a set of bands in materials.

## V. INSTALLATION AND USAGE

In this section, we will show how to install and use the **irvsp** software package. This program is an open source free software package. It is released on Github under the GNU Lesser General Public License, <https://www.gnu.org/licenses/lgpl-3.0.html>, and it can be downloaded directly from the public code archive: [https://github.com/zjwang11/irvsp/blob/master/src\\_irvsp\\_v2.tar.gz](https://github.com/zjwang11/irvsp/blob/master/src_irvsp_v2.tar.gz).

To build and install **irvsp**, only a Fortran 90 compiler is needed. The downloaded **irvsp** software package is likely a compressed file with a **zip** or **tar.gz** suffix. One should uncompress it first, then move into the **src\_irvsp\_v2** folder. After setting up the Fortran compiler in the **Makefile** file, the executable binary **irvsp** can be compiled by typing the following command in the current directory (**src\_irvsp\_v2**):

```
$ ./configure.sh
$ source ~/.bashrc
$ make
```

Before running **irvsp**, the user must provide two consistent files: **WAVECAR** and **OUTCAR**. The two files are generated by the VASP package in fixed format. It is designed to be simple and user friendly. After a running of VASP with **WAVECAR** and **OUTCAR** output, the program **irvsp** can be run immediately. Giving a correct space group number ( $sgn \in [1, 230]$ ) and a set of energy bands (from the  $m$ th band to the  $n$ th band), the program can be executed by the following command:

```
$ irvsp -sg $sgn [-nb $m $n] > outir &
```

## VI. EXAMPLES

Very recently, the codes **vasp2trace** and **CheckTopologicalMat** have been designed for TQC in the Ref. [12]. However, they are not suitable for non-maximal HSK points. In fact, **vasp2trace** is extracted from **irvsp** to interface with **CheckTopologicalMat**. Here, we take topological materials **PdSb<sub>2</sub>** and **Bi** as examples to show how to study topological properties of new materials with **irvsp**. The necessary files for these materials are given as the examples in the archive [src\\_irvsp\\_v2.tar.gz](https://github.com/zjwang11/irvsp/blob/master/src_irvsp_v2.tar.gz).

### A. PdSb<sub>2</sub>

**PdSb<sub>2</sub>** was predicted to be a candidate hosting sixfold-degenerate fermions because of nonsymmorphic symmetry [55, 56]. The crystal of **PdSb<sub>2</sub>** is a cubic structure of SG 205. We adopt the experimental lattice constant  $a$  [57–59] and fully relax the coordinates of inner atomic positions. In the obtained band structure (BS) along the high-symmetry lines (Fig. 5(a)), we note that there is a tiny gap ( $\sim 10$  meV) between two sixfold degeneracies at R. Then, we want to know the corresponding IRs of two sixfold degeneracies and how they are going to evolve under strains. For this purpose, we performed the calculations with different tensile strains (*i.e.*,  $\Delta a/a = 0.31\%$  and  $\Delta a/a = 0.62\%$ ). Their electronic band structures are shown in Figs. 5 (b) and (c), respectively. Comparing with the strain-free BS in Fig. 5(a), we find that the overall BS doesn't change very much, except for the R point. The zoom-in plots around R are shown in lower panels of Fig. 5. The R point is a  $k$ -point with nonsymmorphic symmetry in SG 205, where IRs of the space group can not be expressed as IRs of the corresponding point group multiplied by a phase factor. By running **irvsp**, the IRs at R are obtained. Figs. 6 (a-c) show the results of IRs for the low-energy bands. The number of total electrons is 80 for **PdSb<sub>2</sub>**. It is shown that the energy ordering of electron bands is changed at R under tiny strains.



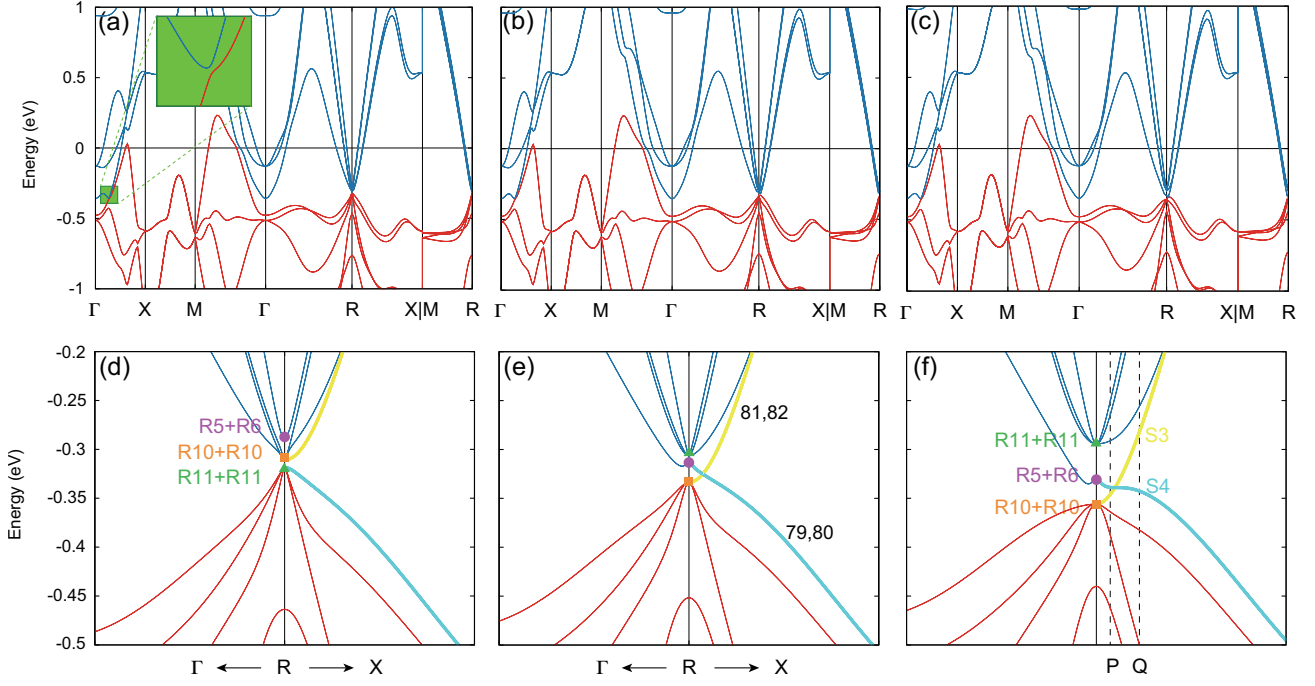


FIG. 5: Electronic band structures of PdSb<sub>2</sub> without strain (a), with 0.31% (b) and 0.62% (c) tensile strains. Panels (d-f) are the zoom-in plots of panels (a-c) near the R point. In our calculations, the total number of electrons is 80. The different IRs at R are labeled by green triangles (R11+R11), orange squares (R10+R10) and purple circles (R5+R6). The two crossing bands along R-X belong to S3 (yellow) and S4 (cyan), respectively. P  $[0.4912 (\frac{2\pi}{a}), 0.5000 (\frac{2\pi}{a}), 0.4912 (\frac{2\pi}{a})]$  and Q  $[0.4722 (\frac{2\pi}{a}), 0.5000 (\frac{2\pi}{a}), 0.4722 (\frac{2\pi}{a})]$  are two points near the crossing point on the R-X line.

The IRs at all the maximal HSK points can be computed directly by `irvsp`. The trace file – `trace.txt` will be generated if only maximal HSK points are given in KPOINTS. By directly comparing these obtained IRs with the EBRs of the TQC theory (released on the BCS) and solving the compatibility relations, we can find that it is a topological insulating phase without strain, while it's a symmetry-enforced semimetallic phase with tiny tensile strains.

To further obtain the crossing points in the system, we computed the IRs along the R-X line (named S  $[u, 0.5, u]$  in units of  $\frac{2\pi}{a}$ ). These points are also non-symmorphic, which are on the boundary of the 3D BZ for SG 205. The CRT for the S point is listed in Fig. S2. For the P and Q points in Fig. 5(f) of the strained crystal, we show the results of obtained IRs in Fig. 7. At the P point, the 79-80 degenerate bands are assigned to “S3+S3”, while 81-82 degenerate bands are assigned to “S4+S4”. However, at the Q point, the results are in the opposite way. Without doing further calculations with a denser kmesh between P and Q points, we can still conclude that it's a real 4-fold crossing along R-X on the BZ boundary, which is robust against SOC. The double degeneracy is due to the presence of TRS. The symmetry #15 is the operator  $g_y \equiv \{M_y | 0\frac{1}{2}\frac{1}{2}\}$ . Therefore, the doubly-degenerate bands have the same  $g_y$  eigenvalue ( $\{S3, S3\}$  or  $\{S4, S4\}$ ), and the 4-fold crossing point along R-X is protected by  $g_y$  symmetry. As a result, the crossing 4-fold points actually form a Dirac nodal ring on the BZ boundary. Considering the full symmetry of SG 205, we conclude that there are three Dirac nodal rings in PdSb<sub>2</sub> with tiny strains, which can be further checked in experiments in the future.

TABLE II: The IRs at maximal HSK points obtained by `irvsp` for Bismuth. “(p)” indicates the degeneracy of the bands, while “[q]” indicates the total number of the computed bands at the  $k$ -point.

HSK	six valence bands
GM	GM8 (2); GM8 (2); GM4 GM5 (2); [6]
T	T9 (2); T8 (2); T6 T7 (2); [6]
F	F3 F4 (2); F5 F6 (2); F5 F6 (2); [6]
L	L3 L4 (2); L5 L6 (2); L5 L6 (2); [6]

(a)									
bnd	ndg	eigval	E	...	15	...	24		
...									
73	2	8.418482	2.00+0.00i	...	-2.00+0.00i	...	-1.00+0.00i	=R8	+ R9
75	6	8.563493	6.00+0.00i	...	2.00+0.00i	...	0.00+0.00i	=R11	+ R11
81	6	8.571287	6.00+0.00i	...	-2.00+0.00i	...	-0.00+0.00i	=R10	+ R10
87	2	8.594609	2.00+0.00i	...	2.00+0.00i	...	1.00+0.00i	=R5	+ R6

(b)									
bnd	ndg	eigval	E	...	15	...	24		
...									
73	2	8.297689	2.00+0.00i	...	-2.00+0.00i	...	-1.00+0.00i	=R8	+ R9
75	6	8.415820	6.00+0.00i	...	-2.00+0.00i	...	0.00+0.00i	=R10	+ R10
81	2	8.440170	2.00+0.00i	...	2.00+0.00i	...	1.00+0.00i	=R5	+ R6
83	6	8.443062	6.00+0.00i	...	2.00+0.00i	...	0.00+0.00i	=R11	+ R11

(c)									
bnd	ndg	eigval	E	...	15	...	24		
...									
73	2	8.178326	2.00+0.00i	...	-2.00+0.00i	...	-1.00+0.00i	=R8	+ R9
75	6	8.262436	6.00+0.00i	...	-2.00+0.00i	...	0.00+0.00i	=R10	+ R10
81	2	8.287815	2.00+0.00i	...	2.00+0.00i	...	1.00+0.00i	=R5	+ R6
83	6	8.324102	6.00+0.00i	...	2.00+0.00i	...	0.00+0.00i	=R11	+ R11

FIG. 6: The IRs at R are determined by the program `irvsp`. The CRT of the R-little group is shown in Fig. S1 in Appendix 4. The first three columns stand for the band indices, degeneracies, and the energies (without subtracting the Fermi energy  $E_F$ ). The following columns indicate the traces (characters) of the corresponding space group operators (listed as “E, 2, ..., 24”). The assigned IR labels are output to the right of the equality sign “=”. The (a), (b), (c) panels are the obtained results for the three crystal structures, respectively.

(a)									
bnd	ndg	eigval	E	...	15	...	...	...	...
1	4	-1.597312	4.00+0.00i	-0.00+0.00i	=S3	+ S3	+ S4	+ S4	
5	4	-1.594935	4.00+0.00i	-0.00+0.00i	=S3	+ S3	+ S4	+ S4	
...									
77	2	8.255055	2.00+0.00i	-2.00+0.00i	=S3	+ S3			
79	2	8.271548	2.00+0.00i	-2.00+0.00i	=S3	+ S3			
81	2	8.279647	2.00+0.00i	2.00+0.00i	=S4	+ S4			
83	2	8.326988	2.00+0.00i	2.00+0.00i	=S4	+ S4			
...									

(b)									
bnd	ndg	eigval	E	...	15	...	...	...	...
1	4	-1.615810	4.00+0.00i	-0.00+0.00i	=S3	+ S3	+ S4	+ S4	
5	4	-1.592474	4.00+0.00i	-0.00+0.00i	=S3	+ S3	+ S4	+ S4	
...									
77	2	8.236502	2.00+0.00i	-2.00+0.00i	=S3	+ S3			
79	2	8.276109	2.00+0.00i	2.00+0.00i	=S4	+ S4			
81	2	8.333843	2.00+0.00i	-2.00+0.00i	=S3	+ S3			
83	2	8.360803	2.00+0.00i	2.00+0.00i	=S4	+ S4			
...									

FIG. 7: The IRs are obtained by `irvsp` for P (a) and Q (b) as depicted in Fig. 5(f).

## B. Bismuth

As aforementioned, with the IRs at maximal HSK points obtained by `irvsp`, we can further check the topology by comparing them with the EBRs of the TQC theory. Here, we will take Bi as an example to briefly introduce the process. The element Bismuth has the rhombohedral structure of SG 166. The maximum HSK points of SG 166 are listed on the BCS, as  $\Gamma$ (GM), T, F, L. After performing the *ab-initio* calculations to obtain the eigen-wavefunctions at maximal HSK points, the obtained IRs of the occupied bands are given in Table II. From the TQC and BCS, the EBRs of SG 166 are obtained, as shown in Fig. 8. As there are only six valence bands, we can find that they do not belong to any EBR induced from the  $9d$  or  $9e$  Wyckoff position. In the EBRs induced from the  $3a$  and  $3b$  Wyckoff positions, we can find that the number of the pairs of F5F6 at F has to be the same as the total number of the IRs GM9 and GM6GM7 at  $\Gamma$ . In Bismuth, the obtained IRs have three IRs of F5F6, but neither GM9 nor GM6GM7. Therefore, the occupied bands of Bismuth can not be expressed as any sum of EBRs in SG 166. In other words, it has to be topological [7].

Wyckoff pos.	3a( $\bar{3}m$ )	3a( $\bar{3}m$ )	3a( $\bar{3}m$ )	3a( $\bar{3}m$ )	3b( $\bar{3}m$ )	3b( $\bar{3}m$ )	3b( $\bar{3}m$ )	3b( $\bar{3}m$ )	9d(2/m)	9d(2/m)	9e(2/m)	9e(2/m)
Band-Rep.	${}^1\bar{E}_g^2\bar{E}_g\uparrow G(2)$	${}^1\bar{E}_u^2\bar{E}_u\uparrow G(2)$	$\bar{E}_{1g}\uparrow G(2)$	$\bar{E}_{1u}\uparrow G(2)$	${}^1\bar{E}_g^2\bar{E}_g\uparrow G(2)$	${}^1\bar{E}_u^2\bar{E}_u\uparrow G(2)$	$\bar{E}_{1g}\uparrow G(2)$	$\bar{E}_{1u}\uparrow G(2)$	${}^1\bar{E}_g^2\bar{E}_g\uparrow G(6)$	${}^1\bar{E}_u^2\bar{E}_u\uparrow G(6)$	${}^1\bar{E}_g^2\bar{E}_g\uparrow G(6)$	${}^1\bar{E}_u^2\bar{E}_u\uparrow G(6)$
Decomposable/ Indecomposable	Indecomposable	Indecomposable	Indecomposable	Indecomposable	Indecomposable	Indecomposable	Indecomposable	Indecomposable	Decomposable	Decomposable	Decomposable	Decomposable
$\Gamma: (0,0,0)$	$\bar{\Gamma}_4\bar{\Gamma}_5(2)$	$\bar{\Gamma}_6\bar{\Gamma}_7(2)$	$\bar{\Gamma}_8(2)$	$\bar{\Gamma}_9(2)$	$\bar{\Gamma}_4\bar{\Gamma}_5(2)$	$\bar{\Gamma}_6\bar{\Gamma}_7(2)$	$\bar{\Gamma}_8(2)$	$\bar{\Gamma}_9(2)$	$\bar{\Gamma}_4\bar{\Gamma}_5(2) \oplus 2\bar{\Gamma}_8(2)$	$\bar{\Gamma}_6\bar{\Gamma}_7(2) \oplus 2\bar{\Gamma}_9(2)$	$\bar{\Gamma}_4\bar{\Gamma}_5(2) \oplus 2\bar{\Gamma}_8(2)$	$\bar{\Gamma}_6\bar{\Gamma}_7(2) \oplus 2\bar{\Gamma}_9(2)$
$T: (0,0,3/2)$	$\bar{\Gamma}_4\bar{\Gamma}_5(2)$	$\bar{\Gamma}_6\bar{\Gamma}_7(2)$	$\bar{\Gamma}_8(2)$	$\bar{\Gamma}_9(2)$	$\bar{\Gamma}_6\bar{\Gamma}_7(2)$	$\bar{\Gamma}_4\bar{\Gamma}_5(2)$	$\bar{\Gamma}_9(2)$	$\bar{\Gamma}_8(2)$	$\bar{\Gamma}_6\bar{\Gamma}_7(2) \oplus 2\bar{\Gamma}_9(2)$	$\bar{\Gamma}_4\bar{\Gamma}_5(2) \oplus 2\bar{\Gamma}_8(2)$	$\bar{\Gamma}_4\bar{\Gamma}_5(2) \oplus 2\bar{\Gamma}_8(2)$	$\bar{\Gamma}_6\bar{\Gamma}_7(2) \oplus 2\bar{\Gamma}_9(2)$
$F: (0,1/2,1)$	$\bar{F}_3\bar{F}_4(2)$	$\bar{F}_5\bar{F}_6(2)$	$\bar{F}_3\bar{F}_4(2)$	$\bar{F}_5\bar{F}_6(2)$	$\bar{F}_3\bar{F}_4(2)$	$\bar{F}_5\bar{F}_6(2)$	$\bar{F}_3\bar{F}_4(2)$	$\bar{F}_5\bar{F}_6(2)$	$\bar{F}_3\bar{F}_4(2) \oplus 2\bar{F}_5\bar{F}_6(2)$	$2\bar{F}_3\bar{F}_4(2) \oplus \bar{F}_5\bar{F}_6(2)$	$\bar{F}_3\bar{F}_4(2) \oplus 2\bar{F}_5\bar{F}_6(2)$	$2\bar{F}_3\bar{F}_4(2) \oplus \bar{F}_5\bar{F}_6(2)$
$L: (-1/2,1/2,1/2)$	$\bar{L}_3\bar{L}_4(2)$	$\bar{L}_5\bar{L}_6(2)$	$\bar{L}_3\bar{L}_4(2)$	$\bar{L}_5\bar{L}_6(2)$	$\bar{L}_3\bar{L}_4(2)$	$\bar{L}_5\bar{L}_6(2)$	$\bar{L}_3\bar{L}_4(2)$	$\bar{L}_5\bar{L}_6(2)$	$2\bar{L}_3\bar{L}_4(2) \oplus \bar{L}_5\bar{L}_6(2)$	$\bar{L}_3\bar{L}_4(2) \oplus 2\bar{L}_5\bar{L}_6(2)$	$\bar{L}_3\bar{L}_4(2) \oplus 2\bar{L}_5\bar{L}_6(2)$	$2\bar{L}_3\bar{L}_4(2) \oplus \bar{L}_5\bar{L}_6(2)$

FIG. 8: A complete list of the EBRs of space group 166 in the presence of SOC. Each EBR is defined by a Maximal Wyckoff site ( $nx$ ) and an IR of its site-symmetry group, which are indicated by the first and second rows, respectively. Then, the following rows present the IRs at the Maximal HSK points.

## VII. CONCLUSIONS

In summary, we present an open-source software package – `irvsp` – that determines the IRs of electronics states in the VASP. It is very user-friendly and is written in Fortran 90/77, showing a powerful function to analyze the IRs for all the  $k$ -points in all 230 SGs, including nonsymmorphic crystals. The associated library – `irrep_bcs.a` – can be interfaced with other DFT packages. We show how to use it to identify IRs and further get the topological property for a new material. As an example, we explore a topological material  $\text{PdSb}_2$ , whose topology is very sensitive to the lattice parameter. Under tiny strains, it is identified as a four-fold Dirac nodal-line metal.

**Acknowledgments** We thank Dr. Peter Blaha and Dr. Luis Elcoro for sharing the character tables of 32 point groups implemented in the WIEN2k package and the character tables of 230 SGs for all  $k$ -points on the BCS. This work was supported by the National Nature Science Foundation of China (Grant No. 11974395), the Strategic Priority Research Program of Chinese Academy of Sciences (Grant No. XDB33000000), the Center for Materials Genome and the CAS Pioneer Hundred Talents Program. Q. S. W. acknowledges the support of NCCR MARVEL.

## APPENDIX

1. tbbbox.in for Bi<sub>2</sub>Se<sub>3</sub>

```

case = soc ! lda or soc

proj:
orbt = 2
ntau = 5
0.39900000 0.39900000 0.39900000 1 3 ! x1, x2, x3, itau, iorbit
0.60100000 0.60100000 0.60100000 1 3
0.20600000 0.20600000 0.20600000 2 3
0.79400000 0.79400000 0.79400000 2 3
0.00000000 0.00000000 0.00000000 2 3
end projections

kpoint:
kmesh = 10
Nk = 4
0.00000000 0.00000000 0.00000000 ! k1: y1,y2,y3
0.50000000 0.50000000 0.50000000 ! k2
0.50000000 0.50000000 0.00000000 ! k3
0.00000000 0.50000000 0.00000000 ! k4
end kpoint_path

unit_cell:
1.194537707 -2.069000000 9.546666657 0.139523990 -0.241662639 0.034916201
1.194537707 2.069000000 9.546666657 0.139523990 0.241662639 0.034916201
-2.389075414 0.000000000 9.546666657 -0.279047979 0.000000000 0.034916201
1 1.000000 0.000000 1.000000 0.000000 0.000000 0.000000 0.000000 0.000000
2 -1.000000 0.000000 1.000000 0.000000 0.000000 0.000000 0.000000 0.000000
3 1.000000 180.000000 0.866025 0.500000 0.000000 0.000000 0.000000 0.000000
4 -1.000000 180.000000 0.866025 0.500000 0.000000 0.000000 0.000000 0.000000
5 1.000000 120.000000 0.000000 0.000000 -1.000000 0.000000 0.000000 0.000000
6 -1.000000 120.000000 0.000000 0.000000 -1.000000 0.000000 0.000000 0.000000
7 1.000000 179.999999 0.000000 1.000000 0.000000 0.000000 0.000000 0.000000
8 -1.000000 179.999999 0.000000 1.000000 0.000000 0.000000 0.000000 0.000000
9 1.000000 120.000000 0.000000 0.000000 1.000000 0.000000 0.000000 0.000000
10 -1.000000 120.000000 0.000000 0.000000 1.000000 0.000000 0.000000 0.000000
11 1.000000 180.000000 0.866025 -0.500000 0.000000 0.000000 0.000000 0.000000
12 -1.000000 180.000000 0.866025 -0.500000 0.000000 0.000000 0.000000 0.000000
end unit_cell

```

TABLE S1: Besides the [src\\_irvsp\\_v2.tar.gz](#) code mainly discussed in the main text, there are more codes developed, which are available in the repository: <https://github.com/zjwang11/irvsp/>. Different versions of the codes are developed based on the different types of the WFs and conventions of the CRTs.

	CRTs		
WFs		PNG	BCS
PW basis		<a href="#">src_irvsp_v1.tar.gz</a>	<a href="#">src_irvsp_v2.tar.gz</a>
TB basis		<a href="#">src_ir2tb_v1.tar.gz</a>	<a href="#">src_ir2tb_v2.tar.gz</a>

## 2. The brief description of ir2tb

Based on the different types of the WFs and conventions of the CRTs, different versions of the codes are developed, as shown in Table S1. The program **ir2tb** is based on the TB WFs. BLAS and LAPACK linear algebra libraries are needed to diagonalize the TB Hamiltonian. To compile **ir2tb**, one needs to copy the library **irrep\_bcs.a** to the folder **src\_ir2tb\_v2** and type the following command:

```
$ make
```

The program **ir2tb** needs two input files: **tbbox.in** and **case\_hr.dat**. The **case\_hr.dat** file, containing the TB parameters in Wannier90 format [46], may be generated by the software Wannier90 [47] with symmetrization [50], or generated by users with a toy TB model, or generated from Slater-Koster method [51] or a discretization of  $k \cdot p$  model onto a lattice [52].

The **tbbox.in** file provides detailed information about the TB Hamiltonian (*i.e.*, the **case\_hr.dat** file), which is summarized in Table S2. It is an essential input for the program **ir2tb**. The tag **case = lda** (**case = soc**) indicates that the TB Hamiltonian does not (does) have the SOC effect. The **lda/soc\_hr.dat** is needed accordingly. In the **proj** block, **orbt = 1** or **2** indicates the convention of the local orbital ordering on each atom. The local orbitals in convention 1 are listed in Table S3, while those in convention 2 are in the order as implemented in Wannier90. **ntau** indicates the total number of the atoms in the TB Hamiltonian, which also means how many lines follow in this block. The local orbitals of the TB Hamiltonian are provided by: **x1,x2,x3, itau, iorbit**. **x1,x2,x3** stand for the positions of atoms:  $\tau_i = (x_1\mathbf{t}_1, x_2\mathbf{t}_2, x_3\mathbf{t}_3)$ ; **itau** stand for the kinds of atoms; and **iorbit** stand for the total numbers of local orbitals on different atoms. So far, **iorbit** is limited to the values of  $\{1, 3, 5, 4, 6, 7, 8, 9\}$ , whose detailed orbital informations are provided in Table S3. In the case of **case = soc**, the local orbitals will be doubled automatically: the first half are spin-up and the second half are spin-down. In the **kpoint** block, the  $k$ -path is given as  $k_1 - k_2 - \dots - k_N$  with **kmesh** points on each segment. The **unit\_cell** block gives the lattice vectors and reciprocal lattice vectors in first three lines, followed by space group operators, which are the same lines as **irvsp** reads in OUTCAR file.

TABLE S2: A brief summary of **tbbox.in**.

Comments	Descriptions
! lda or soc	lda: nspin=1 (without SOC); soc: nspin=2 (with SOC)
! x1,x2,x3,itau,iorbit	defining $\tau_i = (x_1\mathbf{t}_1, x_2\mathbf{t}_2, x_3\mathbf{t}_3)$ , $\text{iorbit} \in \{1, 3, 4, 5, 6, 7, 8, 9\}$
! k1: y1,y2,y3	defining $\mathbf{k}_1 = (y_1\mathbf{g}_1, y_2\mathbf{g}_2, y_3\mathbf{g}_3)$ ; kpath is along $\mathbf{k}_1 - \mathbf{k}_2 - \dots - \mathbf{k}_N$ .
! blx bly blz; glx gly glz	defining $\mathbf{t}_1 = (b_{1x}\hat{x}, b_{1y}\hat{y}, b_{1z}\hat{z})$ ; $\mathbf{g}_1 = 2\pi(g_{1x}\hat{x}, g_{1y}\hat{y}, g_{1z}\hat{z})$
! SN,Det,omega,nx,ny,nz,v1,v2,v3	defining $\mathcal{O}_s = \{R_s \mathbf{v}_s\}$ with $R_s = \text{Det} \cdot e^{-i\omega(\vec{n} \cdot \vec{L})}$ and $\mathbf{v}_s = (v_1\mathbf{t}_1, v_2\mathbf{t}_2, v_3\mathbf{t}_3)$ . SN stands for the sequential number.

TABLE S3: The local orbitals in convention 1 (*i.e.*, **orbt = 1**) are given below. The vector  $\vec{L}$  is given in Eq. (12) in the main text, while the vectors  $\vec{P}$  and  $\vec{F}$  are given in Eqs. (19–22) in Appendix 2.

iorbit	local orbitals	D-matrices in Eq. (7)
1	$s$	$D^1 = 1$
3	$p_x, p_y, p_z$	$D^3 = \text{Det} \cdot e^{-i\omega(\vec{n} \cdot \vec{L})}$
5	$d_{xy}, d_{yz}, d_{zx}, d_{x^2-y^2}, d_{3z^2-r^2}$	$D^5 = e^{-i\omega(\vec{n} \cdot \vec{P})}$
4	$s, p_x, p_y, p_z$	$D^4 = D^1 \oplus D^3$
6	$s, d_{xy}, d_{yz}, d_{zx}, d_{x^2-y^2}, d_{3z^2-r^2}$	$D^6 = D^1 \oplus D^5$
8	$p_x, p_y, p_z, d_{xy}, d_{yz}, d_{zx}, d_{x^2-y^2}, d_{3z^2-r^2}$	$D^8 = D^3 \oplus D^5$
9	$s, p_x, p_y, p_z, d_{xy}, d_{yz}, d_{zx}, d_{x^2-y^2}, d_{3z^2-r^2}$	$D^9 = D^1 \oplus D^3 \oplus D^5$
7	$f_{xyz}, f_{5x^3-xr^2}, f_{5y^3-yr^2}, f_{5z^3-zr^2}, f_{x(y^2-z^2)}, f_{y(z^2-r^2)}, f_{z(x^2-y^2)}$	$D^7 = \text{Det} \cdot e^{-i\omega(\vec{n} \cdot \vec{F})}$

$$P_x = \begin{pmatrix} 0 & 0 & -i & 0 & 0 \\ 0 & 0 & 0 & -i & -i\sqrt{3} \\ i & 0 & 0 & 0 & 0 \\ 0 & i & 0 & 0 & 0 \\ 0 & i\sqrt{3} & 0 & 0 & 0 \end{pmatrix}; P_y = \begin{pmatrix} 0 & i & 0 & 0 & 0 \\ -i & 0 & 0 & 0 & 0 \\ 0 & 0 & 0 & -i & i\sqrt{3} \\ 0 & 0 & i & 0 & 0 \\ 0 & 0 & -i\sqrt{3} & 0 & 0 \end{pmatrix}; P_z = \begin{pmatrix} 0 & 0 & 0 & 2i & 0 \\ 0 & 0 & i & 0 & 0 \\ 0 & -i & 0 & 0 & 0 \\ -2i & 0 & 0 & 0 & 0 \\ 0 & 0 & 0 & 0 & 0 \end{pmatrix} \quad (19)$$

$$F_x = \begin{pmatrix} 0 & 0 & 0 & 0 & 2i & 0 & 0 \\ 0 & 0 & 0 & 0 & 0 & 0 & 0 \\ 0 & 0 & 0 & \frac{3i}{2} & 0 & 0 & \frac{i\sqrt{15}}{2} \\ 0 & 0 & -\frac{3i}{2} & 0 & 0 & \frac{i\sqrt{15}}{2} & 0 \\ -2i & 0 & 0 & 0 & 0 & 0 & 0 \\ 0 & 0 & 0 & -\frac{i\sqrt{15}}{2} & 0 & 0 & -\frac{i}{2} \\ 0 & 0 & -\frac{i\sqrt{15}}{2} & 0 & 0 & \frac{i}{2} & 0 \end{pmatrix} \quad (20)$$

$$F_y = \begin{pmatrix} 0 & 0 & 0 & 0 & 0 & 2i & 0 \\ 0 & 0 & 0 & -\frac{3i}{2} & 0 & 0 & \frac{i\sqrt{15}}{2} \\ 0 & 0 & 0 & 0 & 0 & 0 & 0 \\ 0 & \frac{3i}{2} & 0 & 0 & \frac{i\sqrt{15}}{2} & 0 & 0 \\ 0 & 0 & 0 & -\frac{i\sqrt{15}}{2} & 0 & 0 & \frac{i}{2} \\ -2i & 0 & 0 & 0 & 0 & 0 & 0 \\ 0 & -\frac{i\sqrt{15}}{2} & 0 & 0 & -\frac{i}{2} & 0 & 0 \end{pmatrix} \quad (21)$$

$$F_z = \begin{pmatrix} 0 & 0 & 0 & 0 & 0 & 0 & 2i \\ 0 & 0 & \frac{3i}{2} & 0 & 0 & \frac{i\sqrt{15}}{2} & 0 \\ 0 & -\frac{3i}{2} & 0 & 0 & \frac{i\sqrt{15}}{2} & 0 & 0 \\ 0 & 0 & 0 & 0 & 0 & 0 & 0 \\ 0 & 0 & -\frac{i\sqrt{15}}{2} & 0 & 0 & -\frac{i}{2} & 0 \\ 0 & -\frac{i\sqrt{15}}{2} & 0 & 0 & \frac{i}{2} & 0 & 0 \\ -2i & 0 & 0 & 0 & 0 & 0 & 0 \end{pmatrix} \quad (22)$$

### 3. The standard settings for POSCAR and maximal HSK points

The standard (default) settings of POSCAR are listed as follows:

- a) unique axis b (cell choice 1) for SGs within the monoclinic system.
- b) obverse triple hexagonal unit cell for R SGs.
- c) the origin choice two - inversion center at (0,0,0) - for the centrosymmetric SGs.

Before one is actually doing the VASP calculations, we strongly suggest that one could run the [phonopy](#) program to get the space group number and standardise the POSCAR with the following command:

```
$ phonopy --tolerance 0.01 --symmetry -c POSCAR
$ cp PPOSCAR POSCAR
```

The maximal HSK points from the BCS are given in the conventional reciprocal lattice vectors, while the lattice vectors in VASP usually are given in the primitive cell. The transformation depends on the type of the lattice. There are only seven different types of lattices, *i.e.*  $P, C, B, A, R, F$  and  $I$ . In the  $X$  type, the primitive lattices ( $\vec{p}_1, \vec{p}_2, \vec{p}_3$ ) are defined by a transformation matrix  $M_X$ .

$$(\vec{p}_1 \ \vec{p}_2 \ \vec{p}_3) = (\vec{c}_1 \ \vec{c}_2 \ \vec{c}_3) \cdot M_X \quad (23)$$

where  $\vec{c}_1, \vec{c}_2$  and  $\vec{c}_3$  are the standard conventional lattices. In the program, all the matrices  $M_X$  are given as follows:

$$M_P = \begin{pmatrix} 1 & 0 & 0 \\ 0 & 1 & 0 \\ 0 & 0 & 1 \end{pmatrix}; M_C = \begin{pmatrix} 0.5 & 0.5 & 0 \\ -0.5 & 0.5 & 0 \\ 0 & 0 & 1 \end{pmatrix}; M_B = \begin{pmatrix} 0.5 & 0 & -0.5 \\ 0 & 1 & 0 \\ 0.5 & 0 & 0.5 \end{pmatrix}; M_A = \begin{pmatrix} 1 & 0 & 0 \\ 0 & 0.5 & -0.5 \\ 0 & 0.5 & 0.5 \end{pmatrix};$$

$$M_R = \begin{pmatrix} 2/3 & -1/3 & -1/3 \\ 1/3 & 1/3 & -2/3 \\ 1/3 & 1/3 & 1/3 \end{pmatrix}; M_F = \begin{pmatrix} 0 & 0.5 & 0.5 \\ 0.5 & 0 & 0.5 \\ 0.5 & 0.5 & 0 \end{pmatrix}; M_I = \begin{pmatrix} -0.5 & 0.5 & 0.5 \\ 0.5 & -0.5 & 0.5 \\ 0.5 & 0.5 & -0.5 \end{pmatrix}.$$



#### 4. The character tables for R-little group and S-little group

Figs. S1 and S2 show the character tables for R-little group and S-little group, respectively. At the  $k$ -point  $[(u, v, w)]$  given in the conventional reciprocal basis, the block  $\begin{matrix} x+iy \\ a & b & c \end{matrix}$  in Fig. S2 corresponds to a complex value of  $(x+iy) \cdot \exp[i\pi(au+bv+cw)]$ .

The k-point name is R  
 24 symmetry operations (module lattice translations) in the R-little group of space sgroup 205  
 We do NOT classify the elements into classes.  
 Table can be found on website: <http://www.cryst.ehu.es/>.

2 R : kname 0.50 0.50 0.50 : given in the conventional basis  
 1 : the exsistance of antiunitary symmetry. 1-exist; 0-no

Reality		1	2	3	4	5	6	7	8	9	10	11	12
0	R1+	2.00+0.00i	0.00+0.00i	0.00+0.00i	0.00+0.00i	0.50+0.87i	0.50+0.87i	0.50+0.87i	0.50+0.87i	0.50-0.87i	-0.50+0.87i	-0.50+0.87i	-0.50+0.87i
0	R1-	2.00+0.00i	0.00+0.00i	0.00+0.00i	0.00+0.00i	0.50+0.87i	0.50+0.87i	0.50+0.87i	0.50+0.87i	0.50-0.87i	-0.50+0.87i	-0.50+0.87i	-0.50+0.87i
-1	R2+	2.00+0.00i	0.00+0.00i	0.00+0.00i	0.00+0.00i	-1.00+0.00i	-1.00+0.00i	-1.00+0.00i	-1.00+0.00i	-1.00+0.00i	1.00+0.00i	1.00+0.00i	1.00+0.00i
-1	R2-	2.00+0.00i	0.00+0.00i	0.00+0.00i	0.00+0.00i	-1.00+0.00i	-1.00+0.00i	-1.00+0.00i	-1.00+0.00i	-1.00+0.00i	1.00+0.00i	1.00+0.00i	1.00+0.00i
0	R3+	2.00+0.00i	0.00+0.00i	0.00+0.00i	0.00+0.00i	0.50-0.87i	0.50-0.87i	0.50-0.87i	0.50-0.87i	0.50+0.87i	-0.50-0.87i	-0.50-0.87i	-0.50-0.87i
0	R3-	2.00+0.00i	0.00+0.00i	0.00+0.00i	0.00+0.00i	0.50-0.87i	0.50-0.87i	0.50-0.87i	0.50-0.87i	0.50+0.87i	-0.50-0.87i	-0.50-0.87i	-0.50-0.87i
1	R4	1.00+0.00i	-1.00+0.00i	-1.00+0.00i	-1.00+0.00i	-1.00+0.00i	-1.00+0.00i	-1.00+0.00i	-1.00+0.00i	-1.00+0.00i	1.00+0.00i	1.00+0.00i	1.00+0.00i
0	R5	1.00+0.00i	-1.00+0.00i	-1.00+0.00i	-1.00+0.00i	0.50-0.87i	0.50-0.87i	0.50-0.87i	0.50-0.87i	0.50+0.87i	-0.50-0.87i	-0.50-0.87i	-0.50-0.87i
0	R6	1.00+0.00i	-1.00+0.00i	-1.00+0.00i	-1.00+0.00i	0.50+0.87i	0.50+0.87i	0.50+0.87i	0.50+0.87i	0.50-0.87i	-0.50+0.87i	-0.50+0.87i	-0.50+0.87i
1	R7	1.00+0.00i	-1.00+0.00i	-1.00+0.00i	-1.00+0.00i	-1.00+0.00i	-1.00+0.00i	-1.00+0.00i	-1.00+0.00i	-1.00+0.00i	1.00+0.00i	1.00+0.00i	1.00+0.00i
0	R8	1.00+0.00i	-1.00+0.00i	-1.00+0.00i	-1.00+0.00i	0.50-0.87i	0.50-0.87i	0.50-0.87i	0.50-0.87i	0.50+0.87i	-0.50-0.87i	-0.50-0.87i	-0.50-0.87i
0	R9	1.00+0.00i	-1.00+0.00i	-1.00+0.00i	-1.00+0.00i	0.50+0.87i	0.50+0.87i	0.50+0.87i	0.50+0.87i	0.50-0.87i	-0.50+0.87i	-0.50+0.87i	-0.50+0.87i
0	R10	3.00+0.00i	1.00+0.00i	1.00+0.00i	1.00+0.00i	0.00+0.00i	0.00+0.00i	0.00+0.00i	0.00+0.00i	0.00+0.00i	0.00+0.00i	0.00+0.00i	0.00+0.00i
1	R11	3.00+0.00i	1.00+0.00i	1.00+0.00i	1.00+0.00i	0.00+0.00i	0.00+0.00i	0.00+0.00i	0.00+0.00i	0.00+0.00i	0.00+0.00i	0.00+0.00i	0.00+0.00i
<hr/>													
		13	14	15	16	17	18	19	20	21	22	23	24
		2.00+0.00i	0.00+0.00i	0.00+0.00i	0.00+0.00i	0.50+0.87i	0.50+0.87i	0.50+0.87i	0.50+0.87i	0.50-0.87i	-0.50+0.87i	-0.50+0.87i	-0.50+0.87i
		-2.00+0.00i	0.00+0.00i	0.00+0.00i	0.00+0.00i	-0.50-0.87i	-0.50-0.87i	-0.50-0.87i	-0.50-0.87i	-0.50+0.87i	0.50-0.87i	0.50-0.87i	0.50-0.87i
		2.00+0.00i	0.00+0.00i	0.00+0.00i	0.00+0.00i	-1.00+0.00i	-1.00+0.00i	-1.00+0.00i	-1.00+0.00i	-1.00+0.00i	1.00+0.00i	1.00+0.00i	1.00+0.00i
		-2.00+0.00i	0.00+0.00i	0.00+0.00i	0.00+0.00i	1.00+0.00i	1.00+0.00i	1.00+0.00i	1.00+0.00i	1.00+0.00i	-1.00+0.00i	-1.00+0.00i	-1.00+0.00i
		2.00+0.00i	0.00+0.00i	0.00+0.00i	0.00+0.00i	0.50-0.87i	0.50-0.87i	0.50-0.87i	0.50-0.87i	0.50+0.87i	-0.50-0.87i	-0.50-0.87i	-0.50-0.87i
		-2.00+0.00i	0.00+0.00i	0.00+0.00i	0.00+0.00i	-0.50+0.87i	-0.50+0.87i	-0.50+0.87i	-0.50+0.87i	-0.50-0.87i	0.50+0.87i	0.50+0.87i	0.50+0.87i
		1.00+0.00i	-1.00+0.00i	-1.00+0.00i	-1.00+0.00i	-1.00+0.00i	-1.00+0.00i	-1.00+0.00i	-1.00+0.00i	-1.00+0.00i	1.00+0.00i	1.00+0.00i	1.00+0.00i
		1.00+0.00i	-1.00+0.00i	-1.00+0.00i	-1.00+0.00i	0.50-0.87i	0.50-0.87i	0.50-0.87i	0.50-0.87i	0.50+0.87i	-0.50-0.87i	-0.50-0.87i	-0.50-0.87i
		1.00+0.00i	-1.00+0.00i	-1.00+0.00i	-1.00+0.00i	0.50+0.87i	0.50+0.87i	0.50+0.87i	0.50+0.87i	0.50-0.87i	-0.50+0.87i	-0.50+0.87i	-0.50+0.87i
		-1.00+0.00i	1.00+0.00i	1.00+0.00i	1.00+0.00i	1.00+0.00i	1.00+0.00i	1.00+0.00i	1.00+0.00i	1.00+0.00i	-1.00+0.00i	-1.00+0.00i	-1.00+0.00i
		-1.00+0.00i	1.00+0.00i	1.00+0.00i	1.00+0.00i	-0.50+0.87i	-0.50+0.87i	-0.50+0.87i	-0.50+0.87i	-0.50-0.87i	0.50+0.87i	0.50+0.87i	0.50+0.87i
		-1.00+0.00i	1.00+0.00i	1.00+0.00i	1.00+0.00i	-0.50-0.87i	-0.50-0.87i	-0.50-0.87i	-0.50-0.87i	-0.50+0.87i	0.50-0.87i	0.50-0.87i	0.50-0.87i
		3.00+0.00i	1.00+0.00i	1.00+0.00i	1.00+0.00i	0.00+0.00i	0.00+0.00i	0.00+0.00i	0.00+0.00i	0.00+0.00i	0.00+0.00i	0.00+0.00i	0.00+0.00i
		-3.00+0.00i	-1.00+0.00i	-1.00+0.00i	-1.00+0.00i	0.00+0.00i	0.00+0.00i	0.00+0.00i	0.00+0.00i	0.00+0.00i	0.00+0.00i	0.00+0.00i	0.00+0.00i

FIG. S1: The CRT of R-little group in the BCS convention.

The k-point name is S  
 2 symmetry operations (module lattice translations) in the S-little group of space sgroup 205  
 We do NOT classify the elements into classes.  
 Table can be found on website: <http://www.cryst.ehu.es/>.

12 S : kname u 0.50 u : given in the conventional basis  
 1 : the exsistance of antiunitary symmetry. 1-exist; 0-no

Reality		1	15
0	S1	1.00+0.00i	1.00+0.00i
			1.0 0.0 0.0
0	S2	1.00+0.00i	-1.00+0.00i
			1.0 0.0 0.0
1	S3	1.00+0.00i	0.00-1.00i
			1.0 0.0 0.0
1	S4	1.00+0.00i	0.00+1.00i
			1.0 0.0 0.0

FIG. S2: The CRT of S-little group in the BCS convention.

## 5. Other versions of `irvsp`

Four versions of `irvsp` are implemented, as shown in Table S4. Version I works similarly as `irrep` in the WIEN2k package and presents the IRs with PNG symmetries. This version can thus not classify the special  $k$ -points on the boundary of the Brillouin zone of nonsymmorphic crystals, that is, when  $\exp[-ik(R_s \mathbf{v}_t + \mathbf{v}_s)] \neq 1$  for some  $O_s$  and  $O_t$  in  $LG(k)$ . Version II works for those  $k$ -points for nonsymmorphic SGs, where version I doesn't work. Version III combines version I and II. In the (default) version IV, it works for all the  $k$ -points and all 230 SGs in the convention of the BCS notation. One can use an optional flag `-v` to execute other versions of `irvsp`.

```
$ irvsp -sg $sgn [-v $nv] [-nb $m $n] > outir &
```

TABLE S4: Four versions of `irvsp` are implemented. The first column indicates the version number, the second column shows the convention of reference CRTs, and the brief description is followed in the last column.

Version	CRTs	Brief description
version I	PNG	It resembles an analogue of the program <code>irrep</code> in the WIEN2k package.
version II	BCS	It works only for the $k$ -points, where version I does not work.
version III	PNG&BCS	It combines version I and version II.
version IV (default)	BCS	It works for all the $k$ -points and all 230 SGs, including <i>nonsymmorphic</i> SGs. All the IRs are labeled in the convention of the BCS notation.

## 6. The library – `irrep.bcs.a`

The library `irrep.bcs.a` is developed to be interfaced with other DFT packages. Calling the main subroutine `irrep_bcs` can output the IRs labeled in the convention of BCS notation. The program `ir2tb` is an example of calling the library mode. In other words, `ir2tb` has to be compiled by linking to the library `irrep.bcs.a`. The source files of the library `irrep.bcs.a` are released in the public archive: [https://github.com/zjwang11/irvsp/blob/master/lib\\_irrep\\_bcs.tar.gz](https://github.com/zjwang11/irvsp/blob/master/lib_irrep_bcs.tar.gz)

To compile the library, one should first uncompress the archive `lib_irrep_bcs.tar.gz`, then move into the folder `lib_irrep_bcs` and type the following command:

```
$ ./configure.sh
$ source ~/.bashrc
$ make lib
```

The first two commands add an environment variable `IRVSPDATA` and the third command create the library `irrep.bcs.a` in the current folder. There are three main subroutines: `irrep_bcs`, `pw_setup`, `tb_setup` in the library. Their headers and detailed descriptions are given below (`dp = 8`).

```
subroutine irrep_bcs(sgn, num_sym, &
                   rot_input, tau_input, S03_input, SU2_input, &
                   KKK, WK, kphase, &
                   num_bands, m, n, ene_bands, &
                   spinor, dim_basis, num_basis, &
                   coeffa, coeffb, &
                   Gphase_pw, rot_vec_pw, rot_mat_tb)
```

- `integer, intent(in) :: sgn`  
The space group number.
- `integer, intent(in) :: num_sym`  
The number of space-group operations  $O_s \equiv \{R_s | \mathbf{v}_s\}$  (module the integer lattice translations).

- `integer, dimension(3,3,num_sym), intent(in) :: rot_input`  
The rotation part  $R_s$  of space-group operations  $\mathcal{O}_s$  with respect to primitive lattice vectors [*i.e.*, the matrix  $Z$  in Eq. (17)].
- `real(dp), dimension(3,num_sym), intent(in) :: tau_input`  
The translation part  $\mathbf{v}_s$  of space-group operations  $\mathcal{O}_s$  with respect to primitive lattice vectors.
- `real(dp), dimension(3,3,num_sym), intent(in) :: S03_input`  
The  $R_s$  given in Cartesian coordinates [*i.e.*,  $R(\omega, \vec{n})$  in Eq. (12)].
- `complex(dp), dimension(2,2,num_sym), intent(in) :: SU2_input`  
The  $R_s$  given in spin-1/2 space [*i.e.*,  $S(\omega, \vec{n})$  in Eq. (13)].
- `integer, intent(in) :: KKK`  
The sequential number of the given k-point.
- `real(dp), dimension(3), intent(in) :: WK`  
The coordinates of the k-point with respect to primitive reciprocal lattice vectors.
- `complex(dp), dimension(num_sym), intent(in) :: kphase`  
The k-dependent phase factors due to the translation part  $\mathbf{v}_s$  [*i.e.*,  $e^{-i\mathbf{k}\cdot\mathbf{v}_s}$  in Eq. (4) or  $e^{-i(R_s\mathbf{k}\cdot\mathbf{v}_s)}$  in Eq. (9)].
- `integer, intent(in) :: num_bands`  
The total number of bands.
- `integer, intent(in) :: m, n`  
The IRs of the set of bands  $[m, n]$  are computed.
- `real(dp), dimension(num_bands), intent(in) :: ene_band`  
The energy of the bands at the k-point.
- `logical, intent(in) :: spinor`  
Set to `.true.` if underlying electronic structure calculation has been performed with spinor wavefunctions.
- `integer, intent(in) :: dim_basis`  
The reserved number of the PW/TB basis.  
If `rot_vec_pw` is given, `dim_basis >= num_basis` for any k-point.  
If `rot_mat_tb` is given, one should set `dim_basis = num_basis`.
- `integer, intent(in) :: num_basis`  
The number of PW or orthogonal TB basis for the given k-point (note: the number of PWs for different k-points are usually different).
- `complex(dp), dimension(dim_basis,num_bands),intent(in) :: coeffa`  
The coefficients of spin-up part of wave functions at the given k-point (note: only `coeffup_basis(1:num_basis, 1:num_bands)` is nonzero).
- `complex(dp), dimension(dim_basis,num_bands),intent(in) :: coeffb`  
The coefficients of spin-down part of wave functions at the given k-point if spinor is `.true.` (note: only `coeffdn_basis(1:num_basis, 1:num_bands)` is nonzero).
- `complex(dp), dimension(dim_basis,num_bands),intent(in), optional :: Gphase_pw`  
The phase factors dependent on the PW vectors [*i.e.*,  $e^{-i\mathbf{G}_{j'}\cdot\mathbf{v}_s}$  in Eq. (4)].
- `integer(dp), dimension(dim_basis,num_bands),intent(in), optional :: rot_vec_pw`  
The transformation vectors of space-group operations  $\mathcal{O}_s$ , which send the  $j$ th PW to the  $j'$ th PW [*i.e.*,  $\mathbf{G}_{j'} \equiv R_s(\mathbf{k} + \mathbf{G}_j) - \mathbf{k}$  in Eq. (4)].
- `integer(dp), dimension(dim_basis,dim_basis,num_bands),intent(in), optional :: rot_mat_tb`  
The transformation matrices of space-group operations  $\mathcal{O}_s$  in the orthogonal TB basis [*i.e.*,  $\overline{V(R_s\mathbf{k} - \mathbf{k})D}$  in Eq. (9)].

```

subroutine pw_setup(WK, lattice, &
                  num_sym, det, angle, axis, tau, &
                  dim_basis, num_basis, Gvec, &
                  rot, S03, SU2, &
                  kphase, Gphase_pw, rot_vec_pw)

```

- `real(dp), dimension(3), intent(in) :: WK`  
The coordinates of the k-point with respect to primitive reciprocal lattice vectors.
- `real(dp), dimension(3,3), intent(in) :: lattice(3,3)`  
The primitive lattice vectors in Cartesian coordinates [*i.e.*,  $(\mathbf{t}_1, \mathbf{t}_2, \mathbf{t}_3)$  in Eq. (14)].
- `integer, intent(in) :: num_sym`  
The number of space-group operations  $\mathcal{O}_s \equiv \{R_s | \mathbf{v}_s\}$  (module the integer lattice translations).
- `real(dp), dimension(num_sym), intent(in) :: det`  
The determination of the rotation part  $R_s$  of space-group operations  $\mathcal{O}_s$  [*i.e.*,  $Det$  in Eq. (12)].
- `real(dp), dimension(num_sym), intent(in) :: angle`  
The rotation angle of space-group operations  $\mathcal{O}_s$  [*i.e.*,  $\omega$  in Eq. (12)].
- `real(dp), dimension(3,num_sym), intent(in) :: axis`  
The rotation axis of space-group operations  $\mathcal{O}_s$  in Cartesian coordinates [*i.e.*,  $\vec{n}$  in Eq. (12)].
- `real(dp), dimension(3,num_sym), intent(in) :: tau`  
The translation part  $\mathbf{v}_s$  of space-group operations  $\mathcal{O}_s$  with respect to primitive lattice vectors.
- `integer, intent(in) :: dim_basis`  
The reserved number of the PW basis (`dim_basis`  $\geq$  `num_basis`).
- `integer, intent(in) :: num_basis`  
The number of the PWs for the given k-point (note: `num_basis` for different k-points are usually different).
- `integer, dimension(3, dim_basis), intent(in) :: Gvec`  
The plane-wave G-vector with respect to reciprocal lattice vectors [*i.e.*,  $\mathbf{G}_j$  in Eq. (3)].
- `integer, dimension(3,3,num_sym), intent(out) :: rot`  
The rotation part  $R_s$  of  $\mathcal{O}_s$  with respect to primitive lattice vectors [*i.e.*, the matrix  $Z$  in Eq. (17)].
- `real(dp), dimension(3,3,num_sym), intent(out) :: S03`  
The  $R_s$  given in Cartesian coordinates [*i.e.*,  $R(\omega, \vec{n})$  in Eq. (12)].
- `complex(dp), dimension(2,2,num_sym), intent(out) :: SU2`  
The  $R_s$  given in spin-1/2 space [*i.e.*,  $S(\omega, \vec{n})$  in Eq. (13)].
- `complex(dp), dimension(num_sym), intent(out) :: kphase`  
The k-dependent phase factors due to the translation part  $\mathbf{v}_s$  [*i.e.*,  $e^{-i\mathbf{k} \cdot \mathbf{v}_s}$  in Eq. (4)].
- `complex(dp), dimension(dim_basis,num_bands), intent(out) :: Gphase_pw`  
The phase factors dependent on the PW vectors [*i.e.*,  $e^{-i\mathbf{G}_{j'} \cdot \mathbf{v}_s}$  in Eq. (4)].
- `integer(dp), dimension(dim_basis,num_bands), intent(out) :: rot_vec_pw`  
The transformation vectors of  $R_s$ , which send the  $j$ th PW to the  $j'$ th PW [*i.e.*,  $\mathbf{G}_{j'} \equiv R_s(\mathbf{k} + \mathbf{G}_j) - \mathbf{k}$  in Eq. (4)].

```

subroutine tb_setup(WK, lattice, &
                  num_sym, det, angle, axis, tau, &
                  num_atom, atom_position, &
                  dim_basis, num_basis, angularmom, orbt, &
                  rot, S03, SU2, &
                  kphase, rot_mat_tb)

```

- `real(dp), dimension(3), intent(in) :: WK`  
The coordinates of the k-point with respect to primitive reciprocal lattice vectors.
- `real(dp), dimension(3,3), intent(in) :: lattice(3,3)`  
The primitive lattice vectors in Cartesian coordinates [*i.e.*,  $(\mathbf{t}_1, \mathbf{t}_2, \mathbf{t}_3)$  in Eq. (14)].
- `integer, intent(in) :: num_sym`  
The number of space-group operations  $\mathcal{O}_s \equiv \{R_s | \mathbf{v}_s\}$  (module the integer lattice translations).
- `real(dp), dimension(num_sym), intent(in) :: det`  
The determination of the rotation part  $R_s$  of space-group operations  $\mathcal{O}_s$  [*i.e.*,  $Det$  in Eq. (12)].
- `real(dp), dimension(num_sym), intent(in) :: angle`  
The rotation angle of space-group operations  $\mathcal{O}_s$  [*i.e.*,  $\omega$  in Eq. (12)].
- `real(dp), dimension(3,num_sym), intent(in) :: axis`  
The rotation axis of space-group operations  $\mathcal{O}_s$  in Cartesian coordinates [*i.e.*,  $\vec{n}$  in Eq. (12)].
- `real(dp), dimension(3,num_sym), intent(in) :: tau`  
The translation part  $\mathbf{v}_s$  of space-group operations  $\mathcal{O}_s$  with respect to primitive lattice vectors.
- `integer, intent(in) :: num_atom`  
The number of atoms in the TB Hamiltonian.
- `real(dp), dimension(3, num_atom), intent(in) :: atom_position`  
The coordinates of atoms with respect to primitive lattice vectors [*i.e.*,  $\tau_\mu$  in Eq. (6)].
- `integer, intent(in) :: dim_basis`  
The reserved number of the TB basis (`dim_basis = num_basis`).
- `integer, intent(in) :: num_basis`  
The number of orthogonal local orbitals for the k-point.
- `integer, dimension(num_atom), intent(in) :: angularmom`  
The local orbital information on each atom. Detailed explanations can be found in Table S3.
- `integer, intent(in) :: orbt`  
The convention of the local orbitals on each atom.  
If `orbt = 1`, local orbitals are in the order of Table S3.  
If `orbt = 2`, local orbitals are in the order as implemented in Wannier90
- `integer, dimension(3,3,num_sym), intent(out) :: rot`  
The rotation part  $R_s$  of  $\mathcal{O}_s$  with respect to primitive lattice vectors [*i.e.*, the matrix  $Z$  in Eq. (17)].
- `real(dp), dimension(3,3,num_sym), intent(out) :: S03`  
The  $R_s$  given in Cartesian coordinates [*i.e.*,  $R(\omega, \vec{n})$  in Eq. (12)].
- `complex(dp), dimension(2,2,num_sym), intent(out) :: SU2`  
The  $R_s$  given in spin-1/2 space [*i.e.*,  $S(\omega, \vec{n})$  in Eq. (13)].
- `complex(dp), dimension(num_sym), intent(out) :: kphase`  
The k-dependent phase factors due to the translation part  $\mathbf{v}_s$  [*i.e.*,  $e^{-i(R_s \mathbf{k} \cdot \mathbf{v}_s)}$  in Eq. (9)].
- `integer(dp), dimension(dim_basis,dim_basis,num_bands), intent(out) :: rot_mat_tb`  
The transformation matrices of  $R_s$  in the orthogonal TB basis [*i.e.*,  $\overline{V(R_s \mathbf{k} - \mathbf{k})D}$  in Eq. (9)].

- 
- [1] B. A. Bernevig, T. L. Hughes, and S.-C. Zhang, *Science* **314**, 1757 (2006).
  - [2] M. König, S. Wiedmann, C. Brüne, A. Roth, H. Buhmann, L. W. Molenkamp, X.-L. Qi, and S.-C. Zhang, *Science* **318**, 766 (2007).
  - [3] C. L. Kane and E. J. Mele, *Physical review letters* **95**, 226801 (2005).
  - [4] B. A. Bernevig and S.-C. Zhang, *Physical review letters* **96**, 106802 (2006).
  - [5] C. Kane and M. Hasan, *Rev. Mod. Phys.* **82**, 3045 (2010).
  - [6] X.-L. Qi and S.-C. Zhang, *Reviews of Modern Physics* **83**, 1057 (2011).
  - [7] F. Schindler, A. M. Cook, M. G. Vergniory, Z. Wang, S. S. Parkin, B. A. Bernevig, and T. Neupert, *Science advances* **4**, eaat0346 (2018).
  - [8] X. Wan, A. M. Turner, A. Vishwanath, and S. Y. Savrasov, *Physical Review B* **83**, 205101 (2011).
  - [9] B. J. Wieder, B. Bradlyn, Z. Wang, J. Cano, Y. Kim, H.-S. D. Kim, A. M. Rappe, C. Kane, and B. A. Bernevig, *Science* **361**, 246 (2018).
  - [10] F. Tang, H. C. Po, A. Vishwanath, and X. Wan, *Nature* **566**, 486 (2019).
  - [11] T. Zhang, Y. Jiang, Z. Song, H. Huang, Y. He, Z. Fang, H. Weng, and C. Fang, *Nature* **566**, 475 (2019).
  - [12] M. Vergniory, L. Elcoro, C. Felser, N. Regnault, B. A. Bernevig, and Z. Wang, *Nature* **566**, 480 (2019).
  - [13] Y. Xu, Z. Song, Z. Wang, H. Weng, and X. Dai, *Phys. Rev. Lett.* **122**, 256402 (2019), URL <https://link.aps.org/doi/10.1103/PhysRevLett.122.256402>.
  - [14] G. Li, B. Yan, Z. Wang, and K. Held, *Phys. Rev. B* **95**, 035102 (2017), URL <https://link.aps.org/doi/10.1103/PhysRevB.95.035102>.
  - [15] S. Nie, L. Xing, R. Jin, W. Xie, Z. Wang, and F. B. Prinz, *Phys. Rev. B* **98**, 125143 (2018), URL <https://link.aps.org/doi/10.1103/PhysRevB.98.125143>.
  - [16] Y. Qian, S. Nie, C. Yi, L. Kong, C. Fang, T. Qian, H. Ding, Y. Shi, Z. Wang, H. Weng, et al., *npj Computational Materials* **5**, 121 (2019), URL <https://doi.org/10.1038/s41524-019-0260-6>.
  - [17] H. Zhang, C.-X. Liu, X.-L. Qi, X. Dai, Z. Fang, and S.-C. Zhang, *Nature physics* **5**, 438 (2009).
  - [18] Y. Xia, D. Qian, D. Hsieh, L. Wray, A. Pal, H. Lin, A. Bansil, D. Grauer, Y. S. Hor, R. J. Cava, et al., *Nature physics* **5**, 398 (2009).
  - [19] Y. Chen, J. G. Analytis, J.-H. Chu, Z. Liu, S.-K. Mo, X.-L. Qi, H. Zhang, D. Lu, X. Dai, Z. Fang, et al., *science* **325**, 178 (2009).
  - [20] Z. Wang, Y. Sun, X.-Q. Chen, C. Franchini, G. Xu, H. Weng, X. Dai, and Z. Fang, *Physical Review B* **85**, 195320 (2012).
  - [21] Z. Liu, B. Zhou, Y. Zhang, Z. Wang, H. Weng, D. Prabhakaran, S.-K. Mo, Z. Shen, Z. Fang, X. Dai, et al., *Science* **343**, 864 (2014).
  - [22] Z. Wang, H. Weng, Q. Wu, X. Dai, and Z. Fang, *Phys. Rev. B* **88**, 125427 (2013), URL <https://link.aps.org/doi/10.1103/PhysRevB.88.125427>.
  - [23] Z. Liu, J. Jiang, B. Zhou, Z. Wang, Y. Zhang, H. Weng, D. Prabhakaran, S. Mo, H. Peng, P. Dudin, et al., *Nature materials* **13**, 677 (2014).
  - [24] H. Weng, C. Fang, Z. Fang, B. A. Bernevig, and X. Dai, *Physical Review X* **5**, 011029 (2015).
  - [25] S.-M. Huang, S.-Y. Xu, I. Belopolski, C.-C. Lee, G. Chang, B. Wang, N. Alidoust, G. Bian, M. Neupane, C. Zhang, et al., *Nature communications* **6**, 7373 (2015).
  - [26] B. Lv, H. Weng, B. Fu, X. Wang, H. Miao, J. Ma, P. Richard, X. Huang, L. Zhao, G. Chen, et al., *Physical Review X* **5**, 031013 (2015).
  - [27] S.-Y. Xu, I. Belopolski, N. Alidoust, M. Neupane, G. Bian, C. Zhang, R. Sankar, G. Chang, Z. Yuan, C.-C. Lee, et al., *Science* **349**, 613 (2015).
  - [28] T. H. Hsieh, H. Lin, J. Liu, W. Duan, A. Bansil, and L. Fu, *Nature communications* **3**, 982 (2012).
  - [29] Y. Tanaka, Z. Ren, T. Sato, K. Nakayama, S. Souma, T. Takahashi, K. Segawa, and Y. Ando, *Nature Physics* **8**, 800 (2012).
  - [30] Z. Wang, A. Alexandradinata, R. J. Cava, and B. A. Bernevig, *Nature* **532**, 189 (2016).
  - [31] J. Ma, C. Yi, B. Lv, Z. Wang, S. Nie, L. Wang, L. Kong, Y. Huang, P. Richard, P. Zhang, et al., *Science advances* **3**, e1602415 (2017).
  - [32] Z. Zhu, Y. Cheng, and U. Schwingenschlögl, *Physical Review B* **85**, 235401 (2012).
  - [33] H. C. Po, A. Vishwanath, and H. Watanabe, *Nat. Commu.* **8**, 50 (2017), URL <https://www.nature.com/articles/s41467-017-00133-2>.
  - [34] Z. Song, T. Zhang, Z. Fang, and C. Fang, *Nat. Commu.* **9**, 3530 (2018), URL <https://www.nature.com/articles/s41467-018-06010-w>.
  - [35] J. Kruthoff, J. de Boer, J. van Wezel, C. L. Kane, and R.-J. Slager, *Phys. Rev. X* **7**, 041069 (2017), URL <https://link.aps.org/doi/10.1103/PhysRevX.7.041069>.
  - [36] B. Bradlyn, L. Elcoro, J. Cano, M. Vergniory, Z. Wang, C. Felser, M. Aroyo, and B. A. Bernevig, *Nature* **547**, 298 (2017), URL <https://www.nature.com/articles/nature23268>.
  - [37] J. Cano, B. Bradlyn, Z. Wang, L. Elcoro, M. Vergniory, C. Felser, M. Aroyo, and B. A. Bernevig, *Physical Review B* **97**, 035139 (2018).
  - [38] M. Vergniory, L. Elcoro, Z. Wang, J. Cano, C. Felser, M. Aroyo, B. A. Bernevig, and B. Bradlyn, *Physical Review E* **96**, 023310 (2017).



- [39] J. Cano, B. Bradlyn, Z. Wang, L. Elcoro, M. Vergniory, C. Felser, M. Aroyo, and B. A. Bernevig, Physical review letters **120**, 266401 (2018).
- [40] L. Elcoro, B. Bradlyn, Z. Wang, M. G. Vergniory, J. Cano, C. Felser, B. A. Bernevig, D. Orobengoa, G. Flor, and M. I. Aroyo, Journal of Applied Crystallography **50**, 1457 (2017).
- [41] M. I. Aroyo, J. Perez-Mato, D. Orobengoa, E. Tasci, G. De La Flor, and A. Kirov, Bulg. Chem. Commun **43**, 183 (2011).
- [42] H. T. Stokes, B. J. Campbell, and R. Cordes, Acta Crystallographica Section A: Foundations of Crystallography **69**, 388 (2013).
- [43] P. Blaha, K. Schwarz, G. K. Madsen, D. Kvasnicka, and J. Luitz, An augmented plane wave+ local orbitals program for calculating crystal properties (2001).
- [44] C. Persson, *Electronic structure of intrinsic and doped silicon carbide and silicon*, PhD thesis, ISBN 91-7219-442-1 (1999).
- [45] G. Kresse and J. Furthmüller, Phys. Rev. B **54**, 169 (1996).
- [46] N. Marzari, A. A. Mostofi, J. R. Yates, I. Souza, and D. Vanderbilt, Rev. Mod. Phys. **84**, 1419 (2012), URL <https://link.aps.org/doi/10.1103/RevModPhys.84.1419>.
- [47] A. A. Mostofi, J. R. Yates, G. Pizzi, Y.-S. Lee, I. Souza, D. Vanderbilt, and N. Marzari, Computer Physics Communications **185**, 2309 (2014).
- [48] Q. Wu, S. Zhang, H.-F. Song, M. Troyer, and A. A. Soluyanov, Computer Physics Communications **224**, 405 (2018), ISSN 0010-4655, URL <http://www.sciencedirect.com/science/article/pii/S0010465517303442>.
- [49] C. Yue, *Symmetrization of wannier tight-binding models*, [https://github.com/quanshengwu/wannier\\_tools/tree/master/wannhr\\_symm](https://github.com/quanshengwu/wannier_tools/tree/master/wannhr_symm).
- [50] D. Gresch, Q. Wu, G. W. Winkler, R. Häuselmann, M. Troyer, and A. A. Soluyanov, Physical Review Materials **2**, 103805 (2018).
- [51] J. C. Slater and G. F. Koster, Phys. Rev. **94**, 1498 (1954), URL <https://link.aps.org/doi/10.1103/PhysRev.94.1498>.
- [52] M. Willatzen and L. L. Y. Voon, *The kp Method-Electronic Properties of Semiconductors*, vol. 53 (SpringerBerlinHeidelberg,Berlin,Heidelberg, 2009).
- [53] J. F. Cornwell, *Group Theory in Physics [Vol. 1-2]*. (Academic Press, 1984).
- [54] H.-W. Streitwolf, *Group theory in solid-state physics* (Macdonald and Co., 1971).
- [55] B. Bradlyn, J. Cano, Z. Wang, M. Vergniory, C. Felser, R. J. Cava, and B. A. Bernevig, Science **353**, aaf5037 (2016).
- [56] R. Chapai, Y. Jia, W. Shelton, R. Nepal, M. Saghayezhian, J. DiTusa, E. Plummer, C. Jin, and R. Jin, Physical Review B **99**, 161110 (2019).
- [57] J. Pratt, K. Myles, J. Darby Jr, and M. Mueller, Journal of the Less Common Metals **14**, 427 (1968).
- [58] S. Furuseth, K. Selte, A. Kjekshus, P. Nielsen, B. Sjöberg, and E. Larsen, Acta Chem. Scand **19** (1965).
- [59] N. E. Brese and H. G. von Schnering, Zeitschrift für anorganische und allgemeine Chemie **620**, 393 (1994).